ARTIFICIAL NEURAL NETWORK-BASED PROTECTION STRATEGY FOR MICROGRID

Submitted By

Group Members	Roll No
SALAH UDDIN (LEADER)	19EL15
ABDULLAH WAZIR	19EL63
SYED YASIR SHAH	19EL47
SIRAJ AHMED	19EL17
ABDULLAH JAN	19EL32

Batch 2019

Supervised by

DR. SHAZIA BALOCH

Co-supervised by

DR. SAEED ZAMAN

Department of Electrical Engineering

Balochistan University of Engineering and Technology, Khuzdar

Submitted in partial fulfillment of the requirement for the degree of

Bachelor of Electrical Engineering

December 2023

For checking 15-1-2024

DEDICATION

We dedicate our project thesis with the utmost gratitude and love to our beloved parents, who are always praying for us, our teachers, who have always been a source of knowledge and inspiration, and our friends, who helped us along the way until the project was successfully completed.

Every challenging task demands self-work and guidance from elders, especially those who were very dear to us.

For checking
15-1-2024

ABSTRACT

The active distributed networks and a micro grids (MGs) are two examples of smart networks that have lately become crucial to the operation of the electrical system. Electricity is becoming more and more necessary, and MG can help meet this demand. The modern electric grid operates more efficiently by the integration of the electrical power distribution networks and with the architecture of emerging power systems. A MG is made up of loads that are locally connected and directly connected to DG units. It offers high power quality and global energy efficiency. However, with spite of these benefits, it has several technical issues because of its special characteristics and functionality, among which the most important is protection. Protection problems with the MG affect the dependability of the power systems. Therefore, it is imperative to design prompt and effective protection solutions to address crucial difficulties of MG protection. Therefore, this thesis considers signal processing and artificial neural network-based strategy to protect the MG. The wavelet packet transforms-based signal processing technique is used to extract the fault features. Once, the fault data is extracted, the collected dataset is trained and feed into artificial neural network (ANN) for testing to validate the efficiency of the protection strategy. The MATLAB/SIMULINK software environment is used to extract the dataset and Python is used for testing. The results show that the suggested strategy outperforms the alternative protection techniques.

For checking 15-1-2024

ACKNOWLEDGEMENT

We must first and foremost thank Allah for providing us with this opportunity and the abilities to take advantage of it. This thesis is now available in its current form. We truly thank everyone for their guidance and assistance.

We are incredibly appreciative of our parents' attention, support, encouragement, and prayers. Their blessing infuses us with vitality and fortitude. We also honor the sacrifices made by our Martyred and active law enforcement officers, who created a safe space for us to study in peace. These people are unsung heroes.

Our kind project supervisor**, Dr. Shazia Baloch** & co-supervisor **Dr. Saeed Zaman**, has our deepest gratitude for their patience, motivation, vast knowledge, and suggestions throughout this project. Without their support and interest, the project thesis could not have been completed.

We would also like to extend our gratitude to those who has helped us with this project, directly or indirectly.

For checking 15-1-2024

NOMENCLATURE

AND	Active Distribution Network
ANN	Artificial Neural Network
CIDER	Converter Interfaced Distributed Energy Resources
CWT	Continuous Wavelet Transforms
DDC	Dynamic Distribution Companies
DER	Distributed Energy Resources
DG	Distributed Generators
DH	Harmonic Detection
DN	Distribution Network
DWT	Discrete Wavelet Transform
EPS	Electrical Power Systems
FCL	Fault Current Limiter
FT	Fourier Transform
GA	Genetic Algorithm
IGBT	Insulated Gate Bipolar Transistor
MG	Microgrid
MOSFET	Metal-Oxide-Semiconductor Field-Effect Transistor
MPP	Maximum Power Point
MSE	Mean Square Error
OC	Overcurrent
PGF	Power Generation Frameworks
PLL	Phase Locked Loop
PV	Photovoltaic
PWM	Pulse Width Modulation
RL	Reinforcement Learning
SDN	Smart Distribution Networks
SSFCL	Solid-State Fault Current Limiter
THD	Total Harmonic Distortion
VSC	Voltage Source Converter
VSI	Voltage Source Inverter
WPS	Wind Power Systems
WT	Wavelet Transform

For checking 15-1-2024

LIST OF FIGURES

Fig 2.1 MG Protection Scheme 5
Fig 2.2 Differential Protection Scheme 8
Fig 3.1 PV System 13
Fig 3.2 Operation of PV Cell 14
Fig 3.3 Schematic Diagram of a Non-ideal Two-Level VSC 17
Fig 3.4 Transformation Technique 19
Fig 3.5 Control Strategy of DC/AC Inverter 22
Fig 3.6 LCL Filter Per Phase 23
Fig 3.7 IEEE-13 Node Test System 27
Fig 3.8 Decomposition of Detailed & Approximation Coefficient 31
Fig 3.9 ANN Architecture 39
Fig 3.10 Layers of ANN 34
Fig 4.1 Protection Scheme Flow Chart 36
Fig 4.2 PV array output voltage and power 37
Fig 4.3 Phase voltage and current 38
Fig 4.4 DC/AC Inverter 38
Fig 4.5 Current after LCL filter 39
Fig 4.6 Grid Synchronization 39
Fig 4.7 Test Network 40
Fig 4.8 Islanded mode 40
Fig 4.9 Single-phase-to-ground fault 41
Fig 4.10 Line-to-Line fault 41
Fig 4.11 Modal Current 42
Fig 4.12 Wavelet Transform 43

For checking 15-1-2024

Fig 4.13 Total Harmonic Distortion of Current 43
Fig 4.14 ANN Architerature 44
Fig 4.15 ANN Best Validation 44
Fig 4.16 ANN Performance 44
Fig 4.17 ANN Error Histogram 44
Fig 4.18 ANN Training Data 45
Fig 4.19 ANN True and Predicated Label 45

For checking 15-1-2024

LIST OF TABLES

Table 3.1 Solar Panel Specification 15

Table 3.2 Calculated Value of LCL Filter 24

Table 3.3 Line Segment Data..... 26

Table 3.4 Transformer Data 27

Table 3.5 Capacitor Data 27

Table 3.6 IEEE-13 Node Test Simulation Parameter 28

Table 3.7 Grid- Synchronization Parameter 28

Table 3.8 Frequency Range of Detail and Approximation Coefficients..... 32

For checking 15-1-2024

Balochistan University of Engineering and Technology

Khuzdar

Department of Electrical Engineering

Certificate

This confirms that the work presented in this thesis or project on **"Artificial Neural Network-Based Protection Strategy for Microgrid"** is written by the following students themselves under the supervision of **Dr. Shazia Baloch** & co-supervision of **Dr. Saeed Zaman**.

Group Members	Roll No
SALAH UDDIN (LEADER)	19EL15
ABDULLAH WAZIR	19EL63
SYED YASIR SHAH	19EL47
SIRAJ AHMED	19EL17
ABDULLAH JAN	19EL32

This project is submitted to fulfill a portion of the award requirement for the award of "Degree of Bachelors of Engineering" in Electrical Engineering.

Project supervisor **PREC Member 1** **PREC Member 2** **Head of Department**

Date:_____

For check 15-1-2024

TABLE OF CONTENTS

ABSTRACT ..... **iii**
ACKNOWLEDGEMENT ..... **iv**
NOMENCLATURE ..... **v**
LIST OF FIGURES ..... **vi**
LIST OF TABLES ..... **vii**
TABLE OF CONTENTS ..... **x**
1. Introduction 1
1.1 Background 1
1.2 Motivation and Benefits 2
1.3 Problem Statement 3
1.4 Objectives 3
1.5 Project Outcomes 4
1.6 Thesis layout 4
2. Literature Review 5
2.1 Protection Scheme 5
2.1.1 Adaptive protection schemes 5
2.1.2 Distance protection schemes 6
2.1.3 Voltage-based protection 7
2.1.4 Fault current limiter-based scheme 9
2.1.5 Over-current & symmetrical component-based techniques 10
2.1.6 Intelligent protection schemes 11
3. Methodology 12
3.1 Introduction 12
3.2 MATLAB 12
3.3 Simulink 12
3.4 Photovoltaic Cells 12
3.5 Working of PV Cell 13
3.6 Design of PV array 14
3.6.1 Parameters of PV array 14

For checking 15-1-2024

3.7 Three-Phase Inverter Design 16
3.7.1 Power circuit (Two-level) 16
3.8 Model and control of two-level VSC 18
3.8.1 Transformation technique 18
3.8.2 Three-phase system modelling and control using dq-frames 19
3.8.3 Two-level VSC model and control in a dq-frame 20
3.8.4 Phase locked loop (PLL) 21
3.9 Filter Calculations 22
3.10 IEEE-13 Node Test System 25
3.10.1 Basic information 25
3.11 Grid Synchronization 28
3.12 Proposed Scheme 29
3.12.1 Modal Current 29
3.12.2 Wavelet Transform 30
3.12.3 Total Harmonic Distortion of Current 32
3.13 Fault analysis in Microgrid Using Artificial Neural Network Technique 32
4. Simulation Result 36
4.1 Introduction 36
4.2 Results for PV Array 37
4.3 Results for Phase voltage and current 38
4.4 Results for DC/AC Inverter 38
4.5 Results for Grid Synchronization 39
4.6 Results for Test Network 40
4.7 Results for Modal Current 40
4.8 Results for Wavelet Transform 42
4.9 Results for Total Harmonic Distortion of Current 43
4.10 Results for Artificial Neural Network 44
5. Conclusion 46
5.1 Future Work 47
6. REFERENCES 48

For checking 15-1-2024

CHAPTER 1

INTRODUCTION

1.1 Background

Partially delivering electricity to consumers, conventional electrical power systems (EPS) rely on remote transmission and distribution firms. The electrical distribution networks (EDS) in these configurations only allow for one-way power flow. On the other hand, current trends include increased electricity use, increased worries about climate change. However, the recent developments in renewable energy technologies can overcome the conventional electrical power systems problems [1].

Distributed energy resources (DERs) are power production systems that are often integrated into distribution networks' electrical power systems [2],[3]. A number of benefits come with integrating DERs into distribution grids (DG), such as producing energy that is less harmful to the environment, requiring less initial investment, deploying DER systems more quickly, adapting quickly to demand changes, reducing energy waste, and improving power quality and reliability. Intelligent smart distribution networks (SDNs) have replaced traditional passive distribution networks [4],[5]. A passive distribution network is a structure that is limited to moving power in a single direction. Conversely, an entity that possesses the ability to convey energy in both directions, encompassing power produced by DG units, is known as a MG. Due to the bidirectional flow of electricity, the network becomes an active distribution network (DN) upon the addition of DG units. In-depth study is required to develop sophisticated active distribution networks that are capable of flexible and intelligent operation. Future network technologies that result in smart grid or MG installations should be used by dynamic distribution companies (DDC) to harvest clean energy from sustainable DERs. When compared to networks without active management, the use of active networks and efficient management strategies can greatly increase the number of DG unit connections.

For checking 15-1-2024

1.2 Motivation and Benefits

One of the most significant developments in the field of electric power systems is the incorporation of DERs into electrical distribution networks [1]. DERs are relatively small generators, usually with a power output between a few kilowatts (KW) and megawatts (MW) that are integrated with medium- and low-voltage distribution networks. They can supply electricity to nearby loads, or in the event that their generated power exceeds their domestic consumption, they can even export electricity to the utility grid. The bulk of modern DERs are integrated using power-electronic converters. The functioning codes of conventional power systems are being increasingly challenged by the vast proliferation of converter interfaced distributed energy resources (CIDERs), including micro-gas turbines, wind power systems (WPS), solar systems, and battery energy systems. Dispensing a relatively small portion of a distribution network that combines the DERs and maneuvering them in a controlled and purposeful manner is a growing and proficient philosophy of operation to lessen the technological obstacles associated with the extensive penetration of DERs. The MG makes the integration of DERs into distribution networks more trustworthy, efficient, cost-effective, and environmentally friendly, a is one in which the grid and distributed generation are connected simultaneously. There is a lot of scholarly interest in the idea of an MG [6]. Power electronics converters are used in the majority of DERs to interface an MG. This network can quickly rectify power quality issues like as voltage sags, harmonics, and imbalances, even when nonlinear loads are present [7]. Furthermore, the proximity of generation and consumption improves the system's continuity and dependability in meeting the demands of the sensitive loads.

In order to play a significant role in future power systems for a cleaner environment, lower distribution and transmission costs, and to enable practical energy augmentation, an MG is designed to incorporate a large number of CIDERS [8]. The efficient use of limitless renewable energy resources (RER) has the potential to drastically reduce the release of harmful greenhouse gas emissions. Globally, ecological issues are becoming increasingly important. Compact power generators also have many advantages, such as quick construction timelines, low startup costs, and less need for transmission infrastructure. Because of this, several governments are planning to shift away from producing power primarily from coal and toward more ecologically friendly sources of energy.

For checking 15-1-2024

1.3 Problem Statement

The cooperation of DGs and the main grid in an operational DN presents several difficulties, main among them being the protection. This environment raises several important difficulties, such as variations in the short-circuit levels, restrictions on the protective measures, bidirectional current flow, and cases of unjustified tripping [9].

DG integration results in a discernible decrease in the sensitivity of fault current relays. The feeder's higher equivalent impedance is the cause of this. As a result, the relay's working range becomes more limited, making it unable to cover the whole protected line. The result of this insufficiency is protective blindness or compromised protection [11]. MGs that are intended to operate in both islanded and grid connected modes aggravate this impact even more. The efficiency of the relay varies according on the differences in short-circuit levels between different modes.

One particular situation is when a feeder fails and the fault current from a nearby feeder that is connected to the same substation is augmented by the fault current generated by the distributed generation. False tripping is a phenomenon that may occur in this circumstance. This is the unintentional disconnection of the circuit as a result of the protective gear reacting [10].

Distribution networks with a large percentage of DGs are especially vulnerable to interference with their defense mechanisms. This is explained by changes in the power and current flow brought about by the extra fault currents that DGs introduce. The system's dynamics are altered by these additional currents, raising the total short circuit level [9].

1.4 Objectives

Following are the primary objective of this thesis.

1. Modelling of PV array
2. Modelling of DC/AC converter
3. Control strategy of DC/AC converter
4. Designing of LCL filters

For checking 15-1-2024

5. Implementation of IEEE-13 node test system
6. Implementation of the proposed Artificial Neural Network (ANN) in the test network

1.5 Project Outcomes

Creating a thorough simulated evaluation network model that imitates an operational distribution network is the project's main task. The efficient provision of electricity to necessary loads is the goal of this concept. This project's creative defensive technique efficiently locates and fixes errors to guarantee uninterrupted network operation.

1.6 Thesis layout

Several active distribution protection strategies are examined in this thesis. It uses MATLAB / Simulink simulation models to demonstrate a protective strategy. The following is a list of the chapters that comprise the thesis.

Chapter 1: Introduction: examines MG, the problem statement, the objectives, the project outcomes, motivation and advantages, and the thesis layout in addition to providing a quick summary of the topic.

Chapter 2: Literature Review: describes the different protection methods, including the fault current limiter-based scheme, the intelligent protection schemes, the voltage protection, the adaptive protection, the distance protection, the differential protection, and the over-current and symmetrical component-based protection approaches.

Chapter 3: Methodology: explains the fundamentals of MATLAB/Simulink, photovoltaic cells, how they work, how to construct a PV array, how to create a three-phase inverter, how to model an LCL filter, how to model a modified IEEE-13 node system, and how to apply artificial neural network techniques.

Chapter 4: Simulation Results: gives the results and explanations for the Artificial Neural Network system, three-phase inverter, PV array, and LCL filter.

Chapter 5: Conclusion and Future work: concludes the thesis and discusses future research.

For checking 15-1-2024

Chapter 2

Literature Review

2.1 Protection Scheme

This chapter is dedicated to presenting the primary highlights of protection schemes currently employed to tackle MG protection challenges. Some of these protection techniques are given in Fig 2.1.

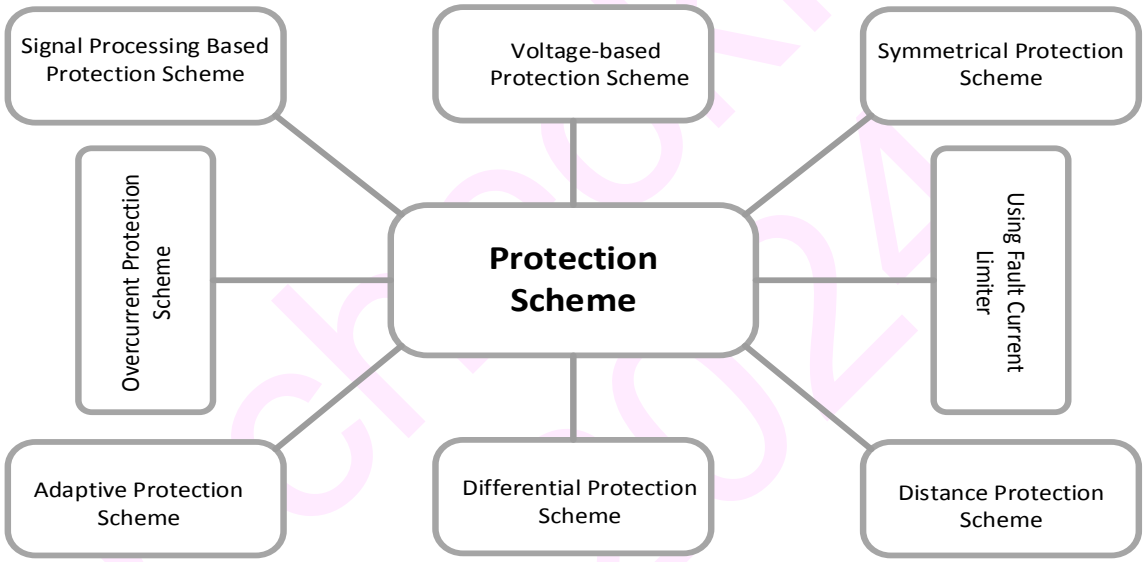

Fig 2.1 MG Protection Scheme

2.1.1 Adaptive protection schemes

Adaptive protection refers to a dynamic and responsive approach in power system protection where the protection settings and parameters are continuously adjusted based on real-time conditions and system characteristics.

A grid-connected system's safe operation can be guaranteed via adaptive protection strategies. These methods automatically adjust the protective relay settings when a MG switches from being isolated to being linked to the main grid. Relay settings are often updated via a networked connection between communication transfers and central processing units. The authors in [5] proposed an adaptive protection method for an MG that does not require communication.

Furthermore, a voltage response for overload and short circuit scenarios was simulated. The simulation results showed that the voltage amplitude dropped in both cases. There was a noticeable decrease in stress in these two cases, but voltage dips were more common in short circuits than in overloads. After then, the problem was found.

Numerical relays were utilized by the developers of [10] to change the previously saved relay settings by the MG scenarios. Every time the DG disengaged from the grid; the relay selected its configuration from a list of options. In [10], a better approach was put out by creating an online technique for figuring out the settings for overcurrent relays. According to the DER state and DG operating mode. All OC relay parameters were automatically changed using the recommended approach.

A directional interlocking adaptive protection scheme is explained in [11]. A central controller upgraded the system relay settings to MG operational mode via a communication link. In [12], a wavelet transform-based multi-agent technique for a distribution network containing DERs was proposed. The network was split up into multiple portions per the plan. Using the communication channel connecting the several agents, MG flaws were located and isolated. The failure direction was identified by utilizing wave coefficients. The system was helpless against letter disappointment. Voltage and current fault components were used to estimate the network impedance. Following that, the impedance of one DG was compared to the utility grid, allowing the instantaneous current relay to automatically determine its settings.

Key issues with adaptive protection strategies include.

- Broad correspondence joins are necessary, although they are not used in practice,
- Complex short-circuit calculations are required for MG operating in multiple modes.
- It entails upgrading and relocating the protective equipment currently utilized in distribution systems.

2.1.2 Distance protection schemes

The electrical impedance of a transmission line is used in relation to its physical length in distance-based protection systems. Devices known as distance relays use this impedance to calculate the

For checking 15-1-2024

distance to a particular, pre-specified location known as a reach point. However, the distance relay did not function as planned or anticipated in circumstances where faults involving the system's grounding happened higher up the line. A directed element was offered in [13] as a solution to the problem. The authors employed negative sequence impedance to differentiate between forward and reverse faults.

The strategy, with its juices and widespread design, was suitable for MG. In [14], an inverse time admittance relay with a radially configured design was explained. The recommended approach could be used to identify low-level fault current. A standard admittance and a predefined value of 1 were compared in order to identify faults. In order to protect MG, a central processing unit-based protection system was employed in [15]. The fault components of a line positive sequence impedance were compared with the positive sequence values prior to the failure in order to determine the fault zone. The proposed structure required a complete upgrade of the current safety devices. Some of the problems that distance relays encounter are as follows:

- Harmonics and transients in the voltage or current signal may cause accuracy problems.
- Errors in the estimation of impedance could be considered a shortcoming obstruction.
- Measuring the impedance of smaller MG lines is time-consuming

2.1.3 Voltage-based protection

In [16], a unique defense tactic that combines traditional overcurrent characteristics with targeted anomaly identification caused by voltage drops is proposed. It involves precise temporal lags. Because the voltage depression in an MG lacks the necessary gradient to distinguish the protection devices, it is impossible to use it alone to detect low levels of fault current. Consequently, it is recommended that more parameters be measured. It is mentioned in [16] that simple device discrimination can be achieved by using precise time delays and current direction. Delays ought to be adjusted according to how sensitive they are to loads or voltage drops. To build suitable discrimination pathways, it is suggested that different delays be chosen for the fault current flow forward and backward. Although utilizing communication channels to coordinate security with automation and control systems may complicate matters, this approach appears promising. An assortment of voltage identification procedures is recommended by the authors of [17] to safeguard

For checking 15-1-2024

networks with low-issue currents. One of the suggested methods uses the Clarke and Park transformations to transform a sequence of instantaneous three-phase utility voltages into a synchronously rotating two-axis coordinate system. To detect disturbances, the voltage that results is compared to a reference value. In the event of an asymmetrical failure, the utility voltage dq components exhibit a ripple above the DC term [16]. Voltage source components can be used for fault detection in low-fault current systems. The values of voltage source components for different types of faults can be calculated thanks to the theory of equivalent sequence network connections in the event of a failure.

Due to its inability to distinguish between fault currents and overload currents in power electronics-interfaced DER units, traditional differential security is unreliable. When there is a system overload, this frequently results in premature tripping. In an isolated micro grid, effective communication between various DGs is essential to ensure appropriate selectivity and precise fault clearance. Improvements are therefore required in order to progress the pilot wireline differential scheme in response to the changing distribution system [10]. If there is a communication breakdown. Voltage and overcurrent (OC) protection have been used as fallback measures. In this plan. Unbalanced loads and switching transients can cause problems, according to the differential protection scheme schematic.

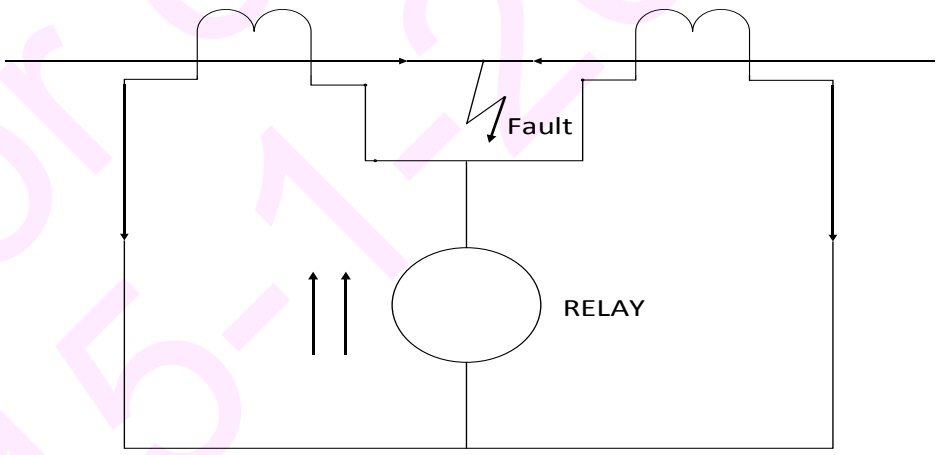

Fig 2.2 Differential Protection Scheme

The authors of [18] explained how MGs might occur and identified two major issues in advance. Comprising control and assurance of voltage and recurrence. This suggested plot makes use of

For checking 15-1-2024

differential assurance. One important benefit of differential protection philosophies is that they are not affected by bidirectional power flow and have a smaller fault current amplitude.

They do, however, have a number of disadvantages, which are listed below:

- They are helpless against letter disappointment.
- Creating a communication channel is very expensive.
- Spikes and unbalanced loads can both reduce efficiency.

2.1.4 Fault current limiter-based scheme

Reducing the short-circuit levels is a useful tactic for reducing the negative effects of DGs on distribution network safety.

The installation of a fault current limiter (FCL) can accomplish this. The FCL is connected in series with the DG unit and acts as an impedance element. This impedance does not change when operations are normal. On the other hand, when a fault occurs, the impedance value rises significantly, limiting the amount of short-circuit current. Crucially, the FCL must quickly and smoothly return to its normal state with negligible impedance after the fault condition is fixed. The writers in [19] look at a number of places where FCL can be connected. It has been shown that the branch where DG is installed is the ideal place to put FCL in order to reduce its impact. One major advantage of having FCL in the same branch as DGs is that there is no need to replace circuit breakers in the branch where DGs are located. According to [20], the functional season of overcurrent transfers can be effectively shortened by introducing FCL in the branch where DG is introduced. The authors of [21] created the reinforcement learning (RL) feed-forward and flux charge model feedback algorithms to shield MG from large currents during voltage sags. The RL algorithm, which is columned by a series inverter that connects the MG to the main network, assigns the distribution feeder a significant virtual RL impedance to reduce transient oscillations and limit line currents. The inverter's available active power is restricted. By contrast, the flux-charge algorithm dampens transient oscillations by using closed-loop control tuning and only adds a virtual inductive impedance that requires no active power. FCL can only be utilized in an MG's regular operating mode, per [22]. The coordination problem was presented as a constrained non-

Forchecking 15-1-2024

linear programming problem, and the authors in [22] showed how to solve it using a genetic algorithm (GA) in both the anchored and unanchored modes. Comparative analyses were first introduced in [23], [24] The primary goal of the OC transfers in these two tests is to completely disregard DG influences. After accounting for DGs, the FCL impedance is then set to allow relay coordination to continue in their presence. The protective plan [25] made use of FCL and communicative linkages to anticipate fault scenarios and configure the protection system accordingly. In order to reduce the impact that DG establishment has on the security configuration of the circulation network in the event of an issue, a solid-state fault current limiter (SSFCL) was proposed in [26]. The voltage-limiting element, current-limiting impedance, fast solid-state switch, mechanical series switch, and voltage-limiting switch comprise the proposed SSFCL. The solid-state components used in the SSFCL cause switching loss. This kind of FCL uses mechanical switches and breakers that have nearly zero closed-circuit losses. The voltage cannot be commutated between the contacts of these switches, despite their ability to operate rapidly. A hybrid FCL was proposed by the authors in [27] as a potential fix for this issue.

2.1.5 Over-current and symmetrical component-based protection techniques:

This includes electrical power and energy frameworks, a robust MG safeguarding arrangement, and traditional over-current safeguarding effectiveness [28]. They suggested a possible way to identify the fault in independent MGs by using measurements from the current symmetrical components. To be more precise, the authors suggested using zero-sequence current detection for upstream single-line-to-ground faults coordinated with imbalanced loads and negative sequence current detection for line-to-line faults. A three-phase plan for communication-aided selectivity was presented in [29]. In step one of the plans, the fault event was identified based on local measurements. Stage two involved the use of inter-breaker communications, and stage three involved the use of a supervisory controller to change the relay settings. The fault detection module and a directional microprocessor-based relay were created by the authors in [30]. The definite-time system was used to identify the relays from the secondary main load side to the MG interface point. Therefore, without prohibiting the use of the MG hardware, the defect may be removed from the generating side of the grading channel more gradually. Upper bounds for the specific time delays on the producing side were established in part because of the significant loads' sensitivity to voltage changes. The maximum duration that electronically connected distributed

For checking 15-1-2024

generators can contribute to a fault current, as well as the dependability of spinning machine-based DGs. The suggested method was notable because it lacked necessary communication links between the relays. The need for communication systems is the main disadvantage of most of the security techniques mentioned above. If a communication system fails, these strategies could jeopardize the coordination of protection.

2.1.6 Intelligent protection schemes

Smart protective systems use data mining techniques to extract latent characteristics from current/voltage signals. SVMs, ANNs, and K-nearest neighbors are examples of sophisticated classifiers that are trained to identify and classify anomalies in micro grids. The original transient current waveforms are extracted for fault localization using mathematical morphology, avoiding detection by plagiarism detection tools in [10]. The wavelet method was used by the authors of [31] to extract the high-frequency components of current and voltage data for radial MG protection. An MG-based boundary wavelet transform protection was developed by the authors in [32].

The wavelet field has been used to calculate the instantaneous and delay elements of the relay. A modified OC relay was then used to identify the faults in the grid tied MGs.

Discrete wavelet transform and a data mining algorithm were used to identify and classify the MG faults [32]. The writers of [33] employed an interval type-2 fuzzy inference system to develop a new MG protection strategy. Different types of fuzzy rules were developed for fault direction identification.

For checking 15-1-2024

Chapter 3

Methodology

3.1 Introduction

The research methodology is thoroughly explained in this section. It delves into the use of MATLAB/SIMULINK for assessing the suggested approach in operating photovoltaic cells, offering detailed insights.

The analysis of PV array functionality, the construction of the DC/AC inverter, the control of the inverter using the dq-frame method, and the implementation of the planned protection strategy using the Artificial Neural Network technique are also explained.

3.2 MATLAB

Matlab, also referred to as Matrix Laboratory, is a software program designed to make handling scientific data more effective [31]. It provides a wide range of built-in functions designed for various research fields, including data analysis, statistics, optimization, and partial differential equation solving.

3.3 Simulink

A software program called Simulink is used to model, simulate, and assess the behavior of systems that display dynamic properties. These systems can function in discrete or continuous time domains, or even both at once [34]. It is possible to simulate both linear and nonlinear systems with Simulink. Moreover, it can manage situations in which various system components need to be sampled or updated at different rates.

3.4 Photovoltaic Cells

A solar photovoltaic system is made up of interconnected modules, each of which has several solar cells arranged in parallel or series. Several modules are connected together to meet the requirement when a single module is unable to supply the required amount of power [26]. To obtain the right

For checking 15-1-2024

voltage levels, a photovoltaic array's module arrangement is frequently carefully selected. The parallel connection of the individual modules in this arrangement allows for the generation of increased current output. In urban environments, these collections of connected modules are attached to rooftops, as shown in Fig 3.1.

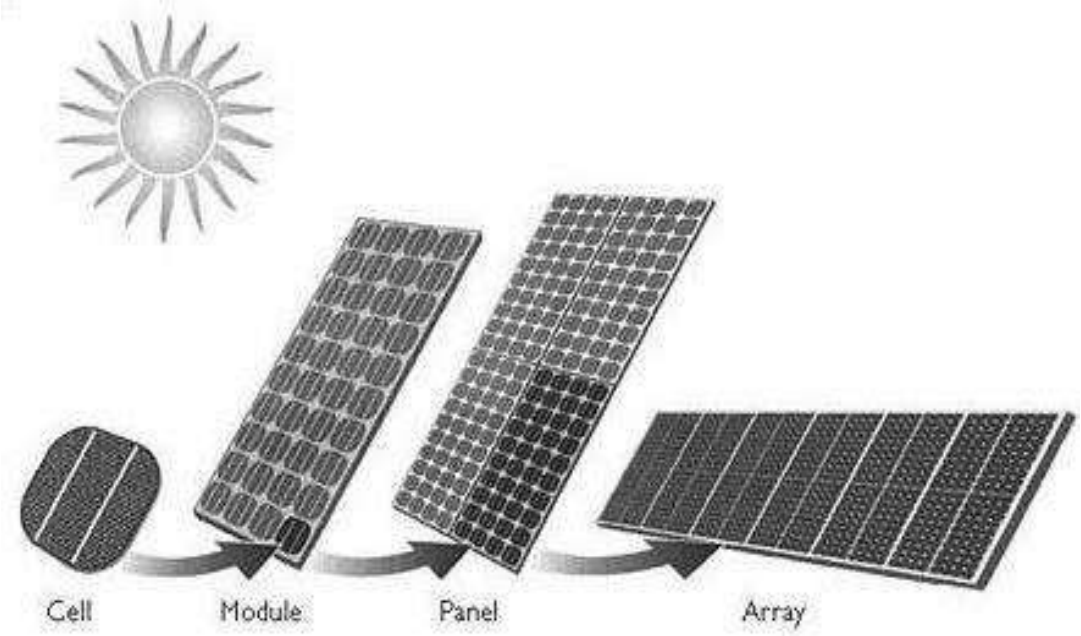

Fig 3.1 PV System. Source :(Ammar A. T. Alkhalidi)

3.5 Working of PV Cell

An intriguing phenomenon happens in a photovoltaic (PV) cell when high-energy photons collide with materials like germanium or silicon. These powerful photons have the ability to shift electrons from the material's conduction band into the valence band by displacing them from their normal locations. They absorb the energy carried by the photons as they move their electrons from the conduction to the valence band [26]. These electrons are kept in a "meta-stable state" for a brief amount of time (usually three to ten seconds) by this energy absorption. The electrons in this meta-stable state are retaining the energy of the photon, akin to a brief pause [32].

This state is temporary, though. These electrons return from the valence band to the conduction band and release the energy they have absorbed after a short period of time, typically 8 to 10 seconds. Light is the manifestation of this energy release. The amazing thing is that power electronic connections are used in the process to transform this light into electrical energy.

Photovoltaic cells are able to produce electricity from sunlight because of this conversion. As illustrated in to Fig 3.2.

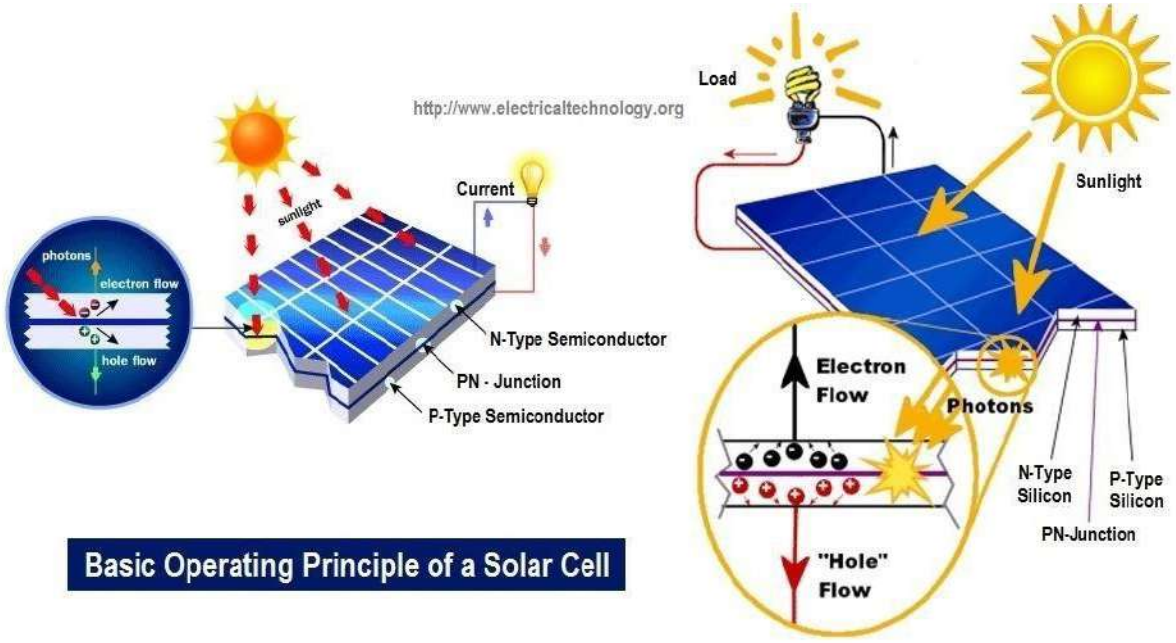

Fig. 3.2: Operation of PV Cell. Source :(K. Nithiyananthan, 2017)

3.6 Design of PV array

MATLAB R2022a was used to create a PV array. The PV array utilized in the project was specified by the company.

3.6.1 Parameters of PV array

- **Modules per string linked in series:**

  There are groups of PV modules in each string. 26 strings are linked in series here. By default, it is Canadian Solar Inc. 300MS CSK.

- **Parallel strings:**

  40 strings are linked in parallel here.

- **Maximum power (*W*):**

Power peak, or the point at which power peaked (V, Vp). There is a formula for Pmax=Pmp × Imp. The 299.92W value is the default.

- **Open-circuit voltage (Voc):**

  When the cluster terminals are open, this voltage is obtained. 39.7V is the default esteem.

- **Short-circuit current (Isc):**

  When exhibit terminals are shorted out, this is the current that is acquired. 9.7A is the default esteem.

- **The Voltage at MPP (Vmp):**

  It represents the voltage at the highest possible power level. 32.6V is the default esteem.

- **Current at MPP (Imp):**

  At its highest power point, the current is. 9.2A is the default esteem.

- Table 3.1 gives the details of the solar panel specifications.

Table 3.1 Solar Panel Specification

Solar Panel Specification			
Series strings	26	Parallel strings	40
Maximum power (W)	299.92W	Cells per module	60
The voltage at maximum power (V)	32.6V	Current at maximum power (A)	9.2A
Open circuit voltage (V)	39.7V	Short circuit current (A)	9.7A

For checking 15-12-2024

3.7 Three-Phase Inverter Design

Inverters are power devices that transform energy source currents and voltages into the necessary sinusoidal voltages and frequencies for grid connection by using semiconductors such as MOSFETs and IGBTs. Even in areas like Pakistan, where the utility frequency is roughly 50 Hz and the rated voltage is about 400V, this procedure is pertinent. Known as voltage source inverters (VSIs), PQ and V−f are the two primary varieties of three-stage inverters.

- **Inverter PQ mode:** A PQ inverter controls actual and reactive power by varying the active and reactive output currents. A voltage-controlled current source is called a PQ inverter [34].
- **Inverter voltage source (VSI) mode:** It controls the voltage and recurrence of the result terminals.

It serves as an inverter for a voltage source [33]. VSI is employed in this thesis. IGBTs are used in a pulse width modulation (PWM) process to generate a series of pulses by turning them on and off. An LCL filter can be used to smooth out the pulses and produce a sinusoidal wave.

3.7.1 Power circuit (Two-level)

A circuit that converts DC power into AC power is called a power inverter. At the output, there are two AC power levels. Six IGBTs and a DC source make up the inputs of the basic circuit. The same leg IGBTs (s_1, s_2), (s_3, s_4), and (s_5, s_6) are separated by 180°. There are 120° separating the upper and lower switches (S_1, S_3, S_5) and (S_4, S_6, S_2). Fig. 3.3 presents a schematic illustration of a two-level VSC. Three half-bridge converters that are identical make up the two-level VSC. Because each of its AC-side terminals can be set to either $+V_{dc}$ or $-V_{dc}$ the converter in Fig 3.5 is referred to as the two-level VSC. The half-span converters' DC sides are connected to and oriented in relation to a common DC-side voltage source. One phase of a three-phase AC system is connected to the AC-side terminal of each half-bridge converter [34]. Power can be transferred back and forth between the three-phase AC system and the DC-side voltage source via the two-level VSC. In this section, it is anticipated that:

- An electrical switch in its conducting state can be described by a voltage drop in series with resistance.

For checking 15/1/2024

- When in the blocking state, an electronic switch simulates an open circuit.
- All semiconductors have a short on-cycle, but the duration of their mood-killing process depends on the following current anomaly.
- The phenomenon of reverse current recovery affects every diode's turn-off process, despite its instantaneous turn-on process.

It is referred to as a two-level VSC because each converter AC-side terminal can assume either of the voltage levels$+V_{dc}$ or $-V_{dc}$ .A common DC-side voltage source is connected in parallel to the half bridge converter's DC sides. Each half-bridge converter's AC-side terminal is connected to one phase of a three-phase AC system. Fig 3.3 displays the three half-bridge converter combinations.

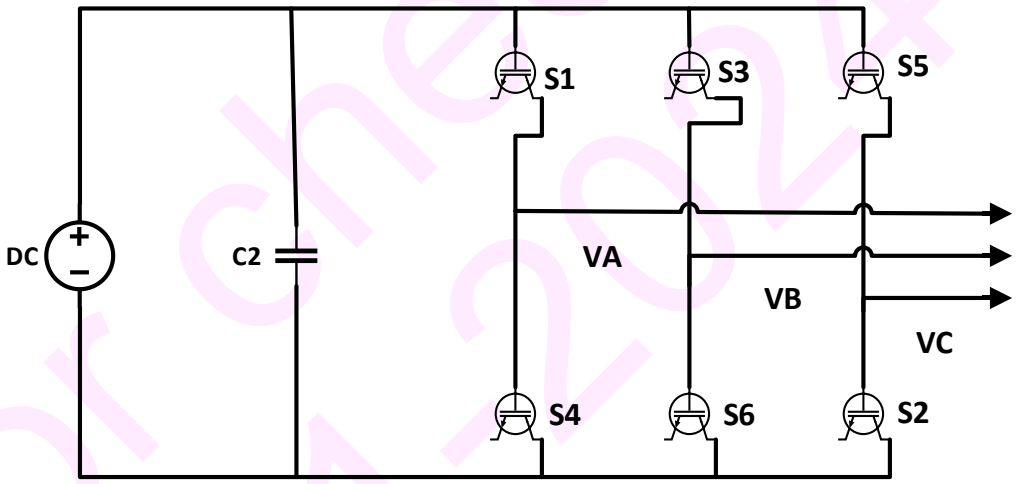

Fig 3.3 Schematic Diagram of a Non ideal Two-Level VSC

A common DC-side voltage source is connected in parallel to the half-bridge converter's DC sides. Each half bridge converter's AC-side terminal is connected to the single-phase of a three-phase AC system. The two-level VSC can act as a bidirectional power-flow channel between the DC-side voltage source or voltage source and the three-phase AC system. An instance of an active AC system is a synchronous machine. One instance of a passive AC system is an RLC load. The letters a, b, and c stand for the half-bridge converters in the two-level VSC of Fig 3.5, and each one is connected to the proper phase of the AC system [33].

For checking 15-1-2024

Claims are made about the pulse-width modulation (PWM) switching method.

$$v't = \bar{v}t - \frac{i}{|i|}ve - r_e, \text{ r}\neq 0 \quad \text{.....(3.1)}$$

$$v't = m(t)\frac{Vdc}{2} - r_{on(t)} \quad \text{.....(3.2)}$$

Where, $v't$ represents the PWM signal. $\bar{v}t$ reference signal.

Three identical half-bridge converters, one for each phase of the AC supply, are found in the two-level VSC shown in Fig 3.3.

The three-terminal voltages on the AC side are as follows:

$$V'_{ta} = m_a(t)\frac{Vdc}{2} - r_{oni_a(t)} \quad \text{.....(3.3)}$$

$$V'_{tb} = m_b(t)\frac{Vdc}{2} - r_{oni_{ab}(t)} \quad \text{.....(3.4)}$$

$$V'_{tc} = m_{ac}(t)\frac{Vdc}{2} - r_{oni_c(t)} \quad \text{.....(3.5)}$$

Where, V'_{ta} is the time-varying output voltage $m_a(t)$ represents the modulation index $r_{oni_a(t)}$ is the time-varying ON-state resistance.

3.8 Model and control of two-level VSC

3.8.1 Transformation technique

A three-phase reference frame can be reduced to a two-phase one using reference frame transformation.

- ABC to αβ is the Clark Transformation (stationary reference frame).
- Park Transformation: from ABC to dq (rotating reference frame).

For checking 15-1-2024

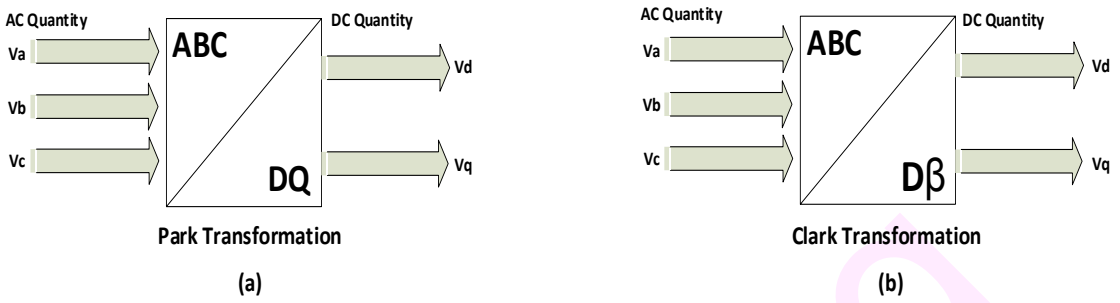

Fig 3.4 Transformation Technique

To facilitate analysis and control, the two primary forms of two-dimensional frames (the dq frame and the αβ-frame) are presented in this section. Using the αβ-frame, the control of a system consisting of three half-bridge converters can be represented as the problem of regulating two equivalent subsystems. Moreover, the concept of instantaneous reactive power can be defined using the αβ frame [34]. When compared to the αβ-frame, the dq-frame has the following advantages.

- If the control is used in the dq-frame, a sinusoidal command tracking problem becomes an analogous DC command tracking problem. Therefore, PI compensators can be used for the control.

- Time-varying, coupled inductances are displayed in models of particular types of electric machinery using the abc-frame. The time-varying inductances are converted into (equivalent) constant parameters if the model is expressed in dq-frame. The dq-frame is frequently used in the construction and analysis of large power system components. Thus, the modeling of VSC systems in the dq-frame enables the application of conventional power system methodologies for analysis and design tasks.

3.8.2 Three-phase system modelling and control using dq-frames

One advantage of the control in dq-frame is that it reduces the required control loop. Frequently, the feed-forward, reference, and feedback signals are sinusoidal time functions. It might be necessary for the compensators to have high orders and for the closed-loop bandwidths to be significantly higher than the frequency of the reference instructions. To deliver a minimal number

For checking 15-1-2024

of steady-state errors and a reasonable performance. It is not simple to design a compensator, particularly if the operating frequency is variable. This issue can be resolved by using the dq-frame-based control. The signals in the dq-frame assume DC waveforms under steady state conditions. This allows for the use of compensators with simpler structural designs and lower dynamic orders. Moreover, zero steady-state tracking error can be achieved by adding integral terms to the compensators. Furthermore, a dq-frame model of a three-phase system is suitable for tasks involving analysis and control design [28].

3.8.3 Two-level VSC model and control in a dq-frame

Because of the sinusoidal variation of the parameters in a current-controlled Voltage Source Converter (VSC) setup, optimizing the performance of compensators is a challenging task. The closed-loop control system must have a large operating range in order to minimize persistent deviations, effectively counteract disturbances, and track commands accurately. This creates a challenging control design problem, particularly for systems with fluctuating frequencies. On the other hand, in the dq-frame, the signals and variables are transformed into equivalent DC quantities. Consequently, the control can be implemented using standard PI compensators, irrespective of the frequency of operation. Furthermore, time-varying characteristics are incorporated into some αβ-frame representations of asymmetrical three-phase systems, and factors such as time-varying inductances in the dq-frame model of a salient-pole synchronous machine complicate control design [34]. When such systems are represented with an appropriate dq-frame, models with constant parameters are generated. Consequently, a VSC system should ideally be represented and controlled in dq-frame. Substituting for

$$m(t) = (m_d + m_q)e^{j\varepsilon(t)} \text{ and } V_t(t) = (m_{dt} + m_{qt})e^{j\varepsilon(t)}$$

$$(m_{dt} + m_{qt})e^{j\varepsilon(t)} = \frac{V_{dc}}{2}(m_d + m_q)e^{j\varepsilon(t)} \quad \text{(3.6)}$$

$$V_{dt} = \frac{V_{dc}}{2} m_d\ (t) \quad \text{(3.7)}$$

$$V_{dt} = \frac{V_{dc}}{2} m_q\ (t) \quad \text{(3.8)}$$

For checking 15-1-2024

Equations (3.7) and (3.8) represent the control strategies for inverters, these equations are part of the modulation scheme. The modulation indices for the DC and Q components are used to control the inverter's output voltage waveform. These equations suggest a simple linear relationship between the modulation indices and the corresponding voltage components, where the voltage for each component is proportional to half of the DC input voltage multiplied by the modulation index for that component [36]. This type of modulation scheme helps control the shape and magnitude of the output voltage waveforms to meet desired specifications and standards for grid-connected systems. describe a relationship where the $d-axis$ and $q-axis$ components of the VSC AC side terminal voltage are directly proportional to the corresponding components of the modulating signal, with a proportionality constant represented by F.

For the two-level VSC, we can break it down into two linear, time-varying subsystems in the $dq-frame$. Each of these subsystems has a transfer function, and this transfer function is characterized by a variable-duration V_{dc} gain or $\frac{V_{dc}}{2}$.

3.8.4 Phase locked loop (PLL)

The PLL delivers the rotation frequency (ω), direct (d), and quadrature (q) voltage or current components by solving the grid's ABC natural components. When the frequency and phase are right, it generates grid voltage and current. Moreover, it can accurately report the grid voltage's frequency and phase angle even in the presence of disturbances. PLL and reference modifications are used to create the three-phase VSI control [33].

On the other hand, the inner current control loop is made using PI controllers. The control of the dq-frame is displayed in Fig 3.5 below.

Forchecking 15-1-2024

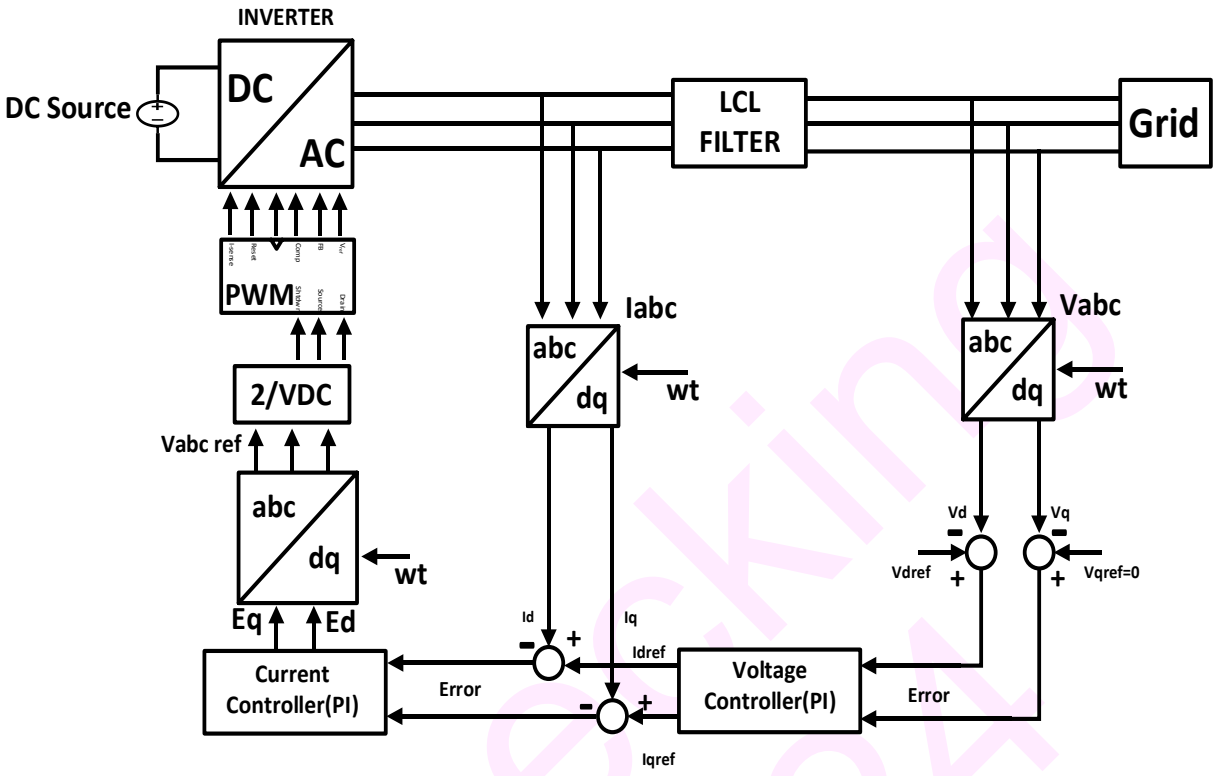

Fig 3.5 Control Strategy DC/AC Inverter

3.9 Filter Calculations

Voltage source inverters (VSI) are used to convert energy from a DC source to an AC output in both stand-alone and grid-connected modes. To lower output current harmonics and enforce a current-like performance for feedback control, a filter is required between a VSI and the grid [19].

Grid-connected inverters and pulse width modulated active rectifiers have been using LCL filters because of their capacity to lower the amount of current distortion fed into the utility grid. Values for LCL filters can be computed as base impedance,

$$Z_b = \frac{(E_n)^2}{P_n} \ldots\ldots\ldots\ldots\ldots\ldots\ldots\ldots\ldots\ldots\ldots\ldots\ldots (3.9)$$

In this case, power is represented by P_n, phase effective voltage by E_n, and base active impedance by Z_b.

For checking 15-1-2024

Base capacitance,

$$C_b = \frac{1}{W_g \times Z_b} \ldots\ldots\ldots\ldots\ldots\ldots\ldots\ldots\ldots\ldots\ldots \quad (3.10)$$

In this case, base capacitance is denoted by C_b, base impedance by Z_b, and grid angular velocity by W_g.

$$I_{max} = \frac{P_n\sqrt{2}}{3V_{ph}} \ldots\ldots\ldots\ldots\ldots\ldots\ldots\ldots\ldots\ldots\ldots\ldots\ldots \quad (3.11)$$

The maximum current in this case is represented by I_{max}, active power by P_n and filter voltage by V_{ph}.

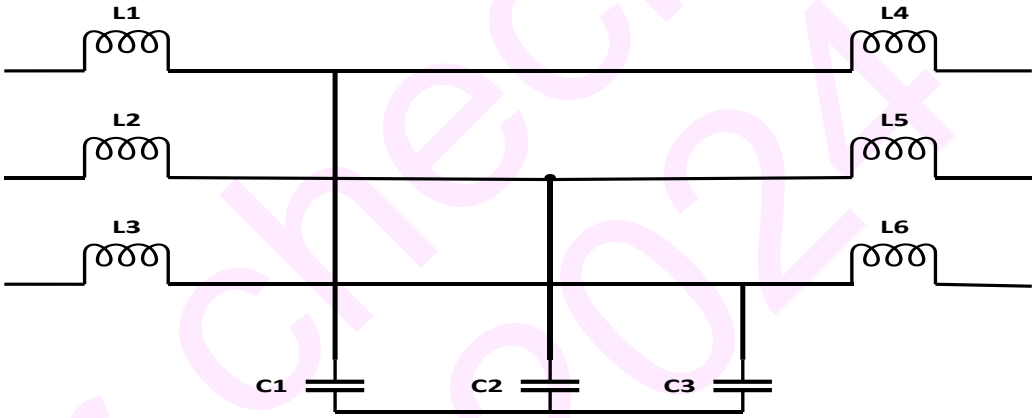

Fig 3.6 LCL Filter Per Phase

In this case, voltage is the maximum current, whereas V_{ph} is the filter and P_n is the active power.

$$V_{ph} = \frac{E_n}{\sqrt{3}} \ldots\ldots\ldots\ldots\ldots\ldots\ldots\ldots\ldots\ldots\ldots\ldots\ldots \quad (3.12)$$

Here, E_n is the one-phase effective voltage and V_{ph} is the filter voltage. if the design parameters permit a 10% variation in the rated current.

$$\Delta I_{Lmax} = \%10 \times I_{max} \ldots\ldots\ldots\ldots\ldots\ldots\ldots\ldots\ldots \quad (3.13)$$

The maximum current is ΔI_{Lmax}, and the current ripple is 10% of the maximum inductor current.

For checking 15-1-2024

$$L_1 = \frac{V_{DC}}{6 \times f_{sw} \times \Delta I_{Lmax}} \ldots\ldots\ldots\ldots\ldots\ldots\ldots\ldots (3.14)$$

Where L_1 is the inductance value on the inverter side, f is the switching frequency, V_{DC} is the dc link voltage, and ΔI_{Lmax} is the current ripple 10% of the maximum inductor current and I_{max} is the maximum current.

The maximum power factor variation of the grid is taken to be 5% in order to construct the filter capacitance. Calculations are used to determine the pertinent parameters for resonance, attenuation, capacitance, and resonance frequency.

$$C_f = 0.05 C_b \ldots\ldots\ldots\ldots\ldots\ldots\ldots\ldots (3.15)$$

Where, C_b is base capacitance , and C_f is filter capacitance .

$$L_2 = \frac{\sqrt{\frac{1}{K_a \hat{} 2} + 1}}{C_f \times W_{sw}^2 * K_a} \ldots\ldots\ldots\ldots\ldots\ldots\ldots\ldots (3.16)$$

Where, K_a = 0.2(20%) → Attenuation factor

Where, L_2 is Grid side inductance, K_a attenuation factor, C_f filter capacitance and W_{sw}. Is switching frequency.

Table 3.2 Calculate value of LCL Filter

Given Parameters	
P_n $(Inverter\ Power)$	$804KW$
E_n $(Grid\ Voltage)$	$220V$
V_{dc} $(DC\ Link\ Voltage)$	$1191V$
F_n $(Grid\ Frequency)$	$50HZ$
F_{sw} $(Switching\ Frequency)$	$15KHZ$
Calculated parameter	
L_1 $(Inverter\ side)$	500 μH
C $(Capacitance)$	500 μF
L_2 $(Grid\ Side)$	500 μH

For checking 2024

Where, L_2 is grid side inductance and K_a is attenuation factor, C_f filter capacitance and W_{sw} angular switching frequency respectively.

$$W_{res} = \sqrt{\frac{L_1+L_2}{L_1 \times L_2 \times C_f}} \dots\dots\dots\dots\dots\dots\dots\dots\dots\dots (3.17)$$

Where, L_2 is grid side inductance, C_f filter capacitance, L_1 is inverter side inductance, W_{res} is resonance angular velocity respectively.

$$F_{res} = \frac{W_{res}}{2\pi} \dots\dots\dots\dots\dots\dots\dots\dots\dots\dots (3.18)$$

Where, F_{res} is resonance frequency and W_{res} is resonance angular velocity.

In order to prevent resonance and reduce some of the ripple factor at the switching frequency, a series resistor link with the capacitor is required. This resistor's impedance must match the filter capacitors at the designated resonance frequency [35]. The damping resistance value can be computed as follows:

$$R_f = \frac{1}{3 \times C_f \times W_{res}} \dots\dots\dots\dots\dots\dots\dots\dots\dots\dots (3.19)$$

Where, W_{res} is resonance angular velocity and C_f filter is capacitance.

3.10 IEEE-13 Node Test System

Using an IEEE-13 node test configuration, the typical characteristics of distribution analysis software operating at a voltage level of 4.16KV have been assessed. With two shunt capacitors, a connected transformer, nine differently distributed loads, and a small overall design, this system functions well even when heavily loaded. The DG source's point of connection is the feeder in the IEEE-13 node test configuration [14].

3.10.1 Basic information of 13 Node Test Model

The following details are applicable to every system

For checking 15-1-2024

Load Concepts

One way to visualize a line segment carrying a load is as an even segment or as a segment connected at a point, similar to a node load (localized load). Additionally, a single-phase or three-phase (symmetrical or asymmetrical) load configuration is an option. For power factor correction (PQ), continuous impedance (Z), or continuous current, single-phase loads can be represented as constant kilowatts (kW) and kilovolt-amperes reactive (kVAr). However, there are two possible configurations for linking three-phase loads: wye and delta. Here, all load data is given in kW and $kVAr$, including the power factor for each phase. The conversion between kW and $kVAr$ for constant current and constant impedance loads should be done assuming rated voltage (1.0 per unit). All three-phases (a-g) will be connected. Phases a, b, and c will be connected as a-b, b-c, and c-a for delta-connected loads, but b-g, and c-g for wye-connected loads. All feeder load tables will only contain loads that are not zero. The total number or increased load is zero [36].

Line Segment Data

Table 3.3 Line Segment Data

Node A	Node B	Length(ft.)	Config.
632	645	500	603
632	633	500	602
633	634	0	XFM-1
645	646	300	603
650	632	2000	601
684	652	800	607
632	671	2000	601
671	684	300	604
671	680	1000	601
671	692	0	Switch
684	611	300	605
692	675	500	606

For checking 15-1-2024

Transformer Data

Table 3.4 Transformer Data

	kVA	kV-high	kV-low	R%	X%
Substation:	5,000	115 – D	4.16 Gr. Y	1	8
XFM -1	500	4.16 – Gr.W	0.48 – Gr.W	1.1	2

Shunt Capacitor

For short-circuit applications, capacitor banks are configured in a variety of ways. These configurations include single-phase connections from line to ground or line to line, as well as three-phase connections in wye or delta configurations. Occasionally, these configurations are combined. The specifications of kVAr on the nameplate indicate that the capacitors are consistent devices with a fixed level of susceptance [13].

Table 3.5 Capacitor Data

Node	Ph-A	Ph-B	Ph-C
	kVAr	kVAr	kVAr
675	200	200	200
611			100
Total	200	200	300

A DG depicted in Fig 3.7 is synchronized with the modified IEEE-13 node system.

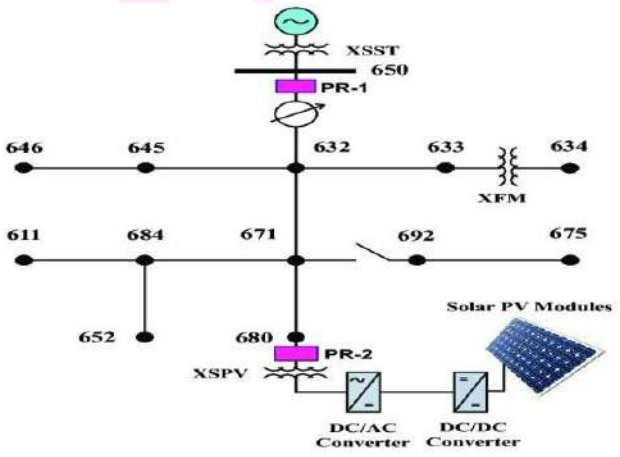

Fig 3.7 IEEE-13 Node Test System

For Checking 1-1-2024

Table 3.6 IEEE-13 Node Test Simulation Parameter

Grid Voltage	4.16KV
Transformer 1 (near Grid)	
MVA	5MVA
Distribution Voltage	3.66KV
Transformer 2 (Connected in feeder)	
MVA Rating	1MVA
Step down voltage	480V
Power demand	
Total Active Power	3.2MVA
Total Reactive Power	1.9MVAR
Total Apparent Power	3.8MVA

3.11 Grid Synchronization

In order for the three-phase inverter system to be synchronized with the grid network, it needs to meet the four fundamental requirements, which are indicated in Fig 3.7.

Table 3.7 Grid- Synchronization Parameter

Parameter	**Description**
Phase Sequence	The phase sequence of the three-phase inverter side must coincide with the three-phases of the grid.
Voltage magnitude	The inverter's sinusoidal voltage and the grid's sinusoidal voltage must have the same magnitude.
Frequency	The frequency of the grid's sinusoidal voltage and the inverter's sinusoidal voltage must match.
Phase angle	The phase angle of the inverter voltage and the grid voltage must match.

For checking 16-12-2024

The most popular technique for synchronizing with the grid is PLL. Open-loop and closed-loop systems are two categories of grid synchronization techniques that have been made possible by recent technological advancements. The amplitude, phase, and frequency of the input signal are all directly detected by open-loop systems. In contrast, closed-loop systems adaptively update the observed parameters through a loop mechanism. Closed loop systems are more accurate since they can handle different circumstances. Since PLL is a closed-loop control system, choosing it intelligently would be wise [39].

3.12 Proposed Scheme

3.12.1 Modal Current

The modal current is created by appropriately combining three-phase currents linearly. It is necessary to consider the currents in all three-phases since transmission line faults can arise in any of the three-phases. Three-phase currents can be transformed into a modal signal to reduce memory usage and computation time [37].

A modal current is the main signal used in the defect detection process. The following examples demonstrate how the modal signal can be created by correctly combining the three-phase voltage or current signals in a linear fashion.

$$Im = \alpha I_a + \beta I_b + \gamma I_c \dots\dots\dots\dots\dots\dots\dots\dots (3.20)$$

$$Vm = \alpha V_a + \beta V_b + \gamma V_c \dots\dots\dots\dots\dots\dots\dots\dots\dots (3.21)$$

The equation 3.20 and 3.21 represents the three-phase current modal signal as I, the observed single-phase currents as I_a, I_b, and I_c, and the modal coefficients as α, β, and γ. The values of 1, -3, and 2 are assigned to the modal coefficients α, β, and γ, respectively.

No two phases can be added or subtracted directly because each phase signal is multiplied by a unique coefficient. The transient content of any two-phase signal combination will not be removed [38].

For checking 15-1-2024

With the exception of their direct summing, which will produce a zero output even after the operation, any combination of the three-phase currents and voltages may be utilized for capacitor switching [33].

Consequently, the modal signal fully preserves the transient components of the three-phase current and voltage signals

3.12.2 Wavelet Transform

Transients in real time Since the high frequency content superimposed on the power frequency signals is typically aperiodic, short term, and non-stationary waveforms, classifying power transients is extremely difficult. In order to extract discriminative features that will aid in distinguishing transients related to an islanding event from those resulting from any other event, such as a temporary fault or the switching of a capacitor bank, wavelet transform is proposed [10]. A popular mathematical tool in many engineering applications, including speech and image processing, is the wavelet transform (WT) [17]. Power system protection, power quality, and partial discharge are just a few of the many uses for WT in the power systems industry. In contrast to Fourier transform (FT), which converts a signal from the time domain to the frequency domain, WT extracts the signal's frequency components while maintaining its time domain properties.

$$X_f = \int_{-\infty}^{\infty} x(t) e^{-j2\pi f t} dt \ldots\ldots\ldots\ldots\ldots\ldots (3.22)$$

Equation (3.22) defines the Fourier transform X_f at the specific frequency f to be the time integral over all time of the product of a given signal $x(t)$ with a complex sinusoid at the specified frequency f. If the signal has a strong component at the particular frequency f if there is a significant component of the signal at frequency f.

Lower frequency components are gradually filtered out as decompositions are performed on higher levels [40]. In addition to breaking down a signal into bands of frequencies, the wavelet transforms (in contrast to the Fourier transform) offers a non-uniform division of the frequency domain, using long windows for low-frequency components and short windows for high-frequency components. Wavelet analysis is the study of expanding functions in terms of a collection of basic functions, or

For checking 15-1-2024

wavelets, which are produced by translating and dilating another wavelet. The continuous wavelet transforms (CWT) of a function v(t) can be computed as [16].

$$CWT(x.y,z) = \frac{1}{\sqrt{a}}\int_{-\infty}^{\infty} x(t)\psi\left(\frac{t-y}{x}\right)dt \ldots\ldots\ldots\ldots\ldots\ldots (3.23)$$

Where, y represents the translation (time shift) and scaling (dilation) constants, respectively, and ψ represents the wavelet function.

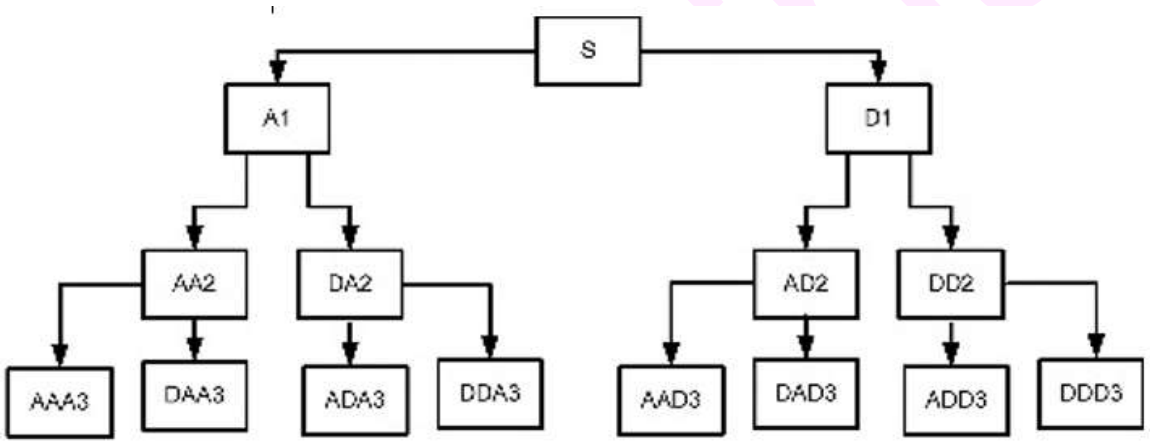

Fig 3.8 Decomposition of Detailed and Approximation Coefficients

One could think of the DWT as a filter bank. To obtain the approximate and detailed coefficients, decomposition is carried out by passing the sampled signal f (t) through a low-pass filter h(n) and a high-pass filter g(n). The signal is first split into an approximation coefficient A_1 with a frequency band of $(\frac{f_s}{4} - 0)$kHz and a detailed coefficient D_1 with a frequency band of $(\frac{f_s}{2} - \frac{f_s}{4})$kHz. The output of both filters is then down sampled by a factor of two. The detailed coefficient is sent to the second stage to generate new coefficients, repeating the process for further decomposition. In the second stage of decomposition, A_2 computes between $(\frac{f_s}{8} - 0)$kHz and D_2 gathers data between $(\frac{f_s}{4} - \frac{f_s}{8})$kHz. Similar to this, A_3 records data between $(\frac{f_s}{16} - 0)$kHz and D_3 records data between $(\frac{f_s}{8} - \frac{f_s}{16})$kHz, where F_s is the original signal sampling frequency. Until the required level of detailed coefficients is obtained, the procedure is repeated for the detailed coefficients [40], [41]. The sampling frequency 3.6 kHz in the case of the suggested scheme,

affects the number of decomposition steps. Details about the comprehensive coefficients acquired through wavelet decomposition are mentioned [44].

Table 3.8 Range of Detail and Approximation Coefficient

Detail Coefficient	Frequency range(kHz)	Approximation Coefficient	Frequency range(kHz)
D_1	(1.8 - 0.9)	A_1	(0.9 – 0)
D_2	(0.9 - 0.45)	A_2	(0.45 – 0)
D_3	(0.45 – 0.225)	A_3	(0.225 – 0)

3.12.3 Total Harmonic Distortion of Current

Signal distortion is indicated by THD. It is regarded as a sensitive feature against the fault and raises the harmonics. It can be current harmonics and is defined as the ratio of total harmonics to the fundamental frequency [39]. The THD of current is calculated with the use of equations and.

$$THD_i = \frac{\sqrt{I_1{}^2 + I_2{}^2 + I_3{}^2 + \cdots I_n{}^2}}{I_1} \quad \text{.....(3.24)}$$

Where, $THDi$ stands for total harmonic distortion of current.

3.13 Fault analysis in MG Using Artificial Neural Network Technique

Artificial Neural Network (ANN)

There are numerous possible uses for artificial neural networks (ANNs) in power system control and operation. Applications where ANN was used as a classifier include load forecasting, fault diagnosis/location, economic dispatch, transient stability, and harmonics analysis [11]. Because ANNs can learn complex mappings, either linear or nonlinear, from the input space to the output space, they are frequently used as classifiers. The following sections provide an explanation of the feed forward artificial neural network's architecture and training methodology.

For checking 15-1-2024

ANN Architecture

A ANN is made up of simple processing units called neurons that work in tandem to solve particular problems. A basic neuron with an input vector P of dimension $R\times1$ is depicted in *Fig 3.9*. Weight W of dimension $1\times R$ is multiplied by the input P. f is a transfer function (also known as the activation function) that takes the argument n and yields the net output a. A bias b is then added to the product WP. The neurons have two programmable parameters: the weight and the bias. The purpose of an artificial neural network (ANN) is to modify these two parameters, W and P, to cause the network to behave in a particular way. As a result, by changing the weight or bias parameters, the network can be trained to perform a specific task [33].

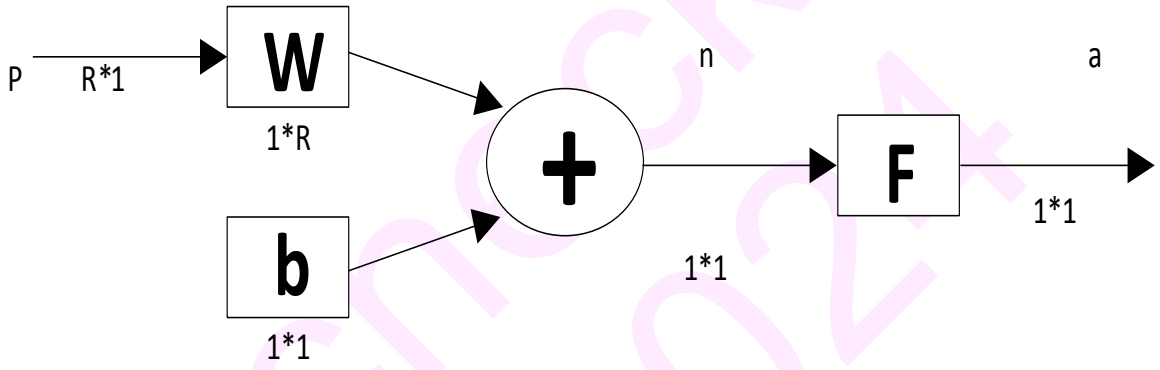

Fig 3.9 ANN Architecture

$$a = f(WP + b) \dots\dots\dots\dots\dots\dots (3.25)$$

Where, W is the weight vector. P is the input vector. b is the bias term. f is the activation function.

Training the ANN

A training algorithm is a process that modifies a network's weights and biases to enable the network to carry out a specific design task. Supervised learning and unsupervised learning are the two primary categories into which the training algorithm falls. ANNs fall under the category of supervised learning. The training data set and associated targets are fed into the model during the training phase. The network is prepared for training once the weights and biases have been initialized. The mean square error, or MSE (the average squared error between the network's

For checking 15-1-2021

outputs, a, and the target outputs is t) then minimized by adjusting the weights and biases. The MSE gradient can be used to accomplish this. Back propagation is a method used to find the gradient descent algorithm [42]. The following is a summary of the steps involved in arriving at the ideal solution:

- To create its output vector, the network first uses the input vector.
- A computation will be made of the discrepancy between the actual target and the obtained target value. The prediction error is the name given to this.
- The gradient (derivatives) of the change in error with respect to changes in weight values will be computed as the error propagates backward through the network.
- In order to minimize error, the weights will be adjusted accordingly. When training multiple layers of neural networks, there are several issues to consider.

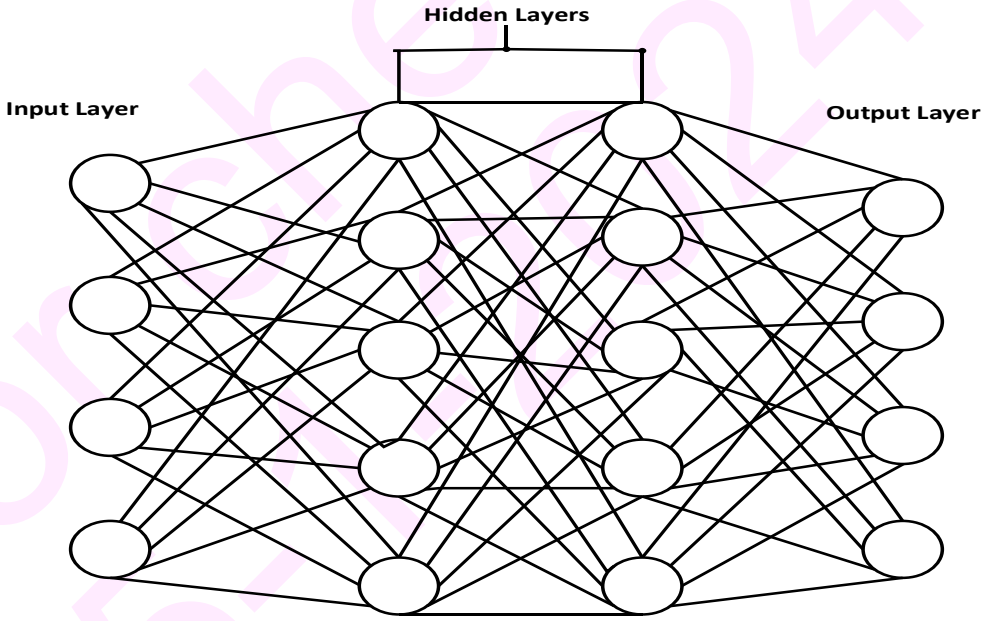

Fig 3.10 Layers of ANN

- Deciding how many hidden layers to include:

  Most problems can be solved with a network that has just one hidden layer [33]. However, in some applications, having more than one hidden layer might lead to learning more quickly. On

Forchecking 15-10-2024

the other hand, networks with multiple hidden layers will have a higher likelihood of convergent to local minima.

- Counting the neurons in the layers that are hidden:

  The network cannot model complex data with a small number of neurons, and the fit that results will be subpar. However, using an excessive number of neurons can lengthen the training period and cause the network to overfit the data. When overfitting takes place, the model fits training data exceptionally well, but it performs poorly when applied to new data. The optimal performance on the validation data should be considered when selecting the number of neurons [42].

For checking 15-1-2024

Chapter 4

Simulation Result

4.1 Introduction

This chapter discusses the simulation results for the PV array and the DC/AC inverter both before and after the LCL filter. Also displayed are the synchronized results of the modified IEEE-13 Node Test system and the DG. The various faults, such as single-phase-to-ground faults, double-line-ground faults, and three-phase-to-ground faults, are categorized, detected, and the ANN result for fault detection is also displayed. The comprehensive flowchart of the proposed fault protection algorithm is depicted in Fig 4.1 To assess the effectiveness and robustness of the introduced fault protection strategy. The implementation of an Artificial Neural Network (ANN) for fault classification further enhances the system's capability to accurately identify and categorize faults. Results obtained from the ANN provide a clear indication of the system's health, allowing for efficient fault detection and subsequent identification, thereby contributing to the overall reliability and performance of the electrical system.

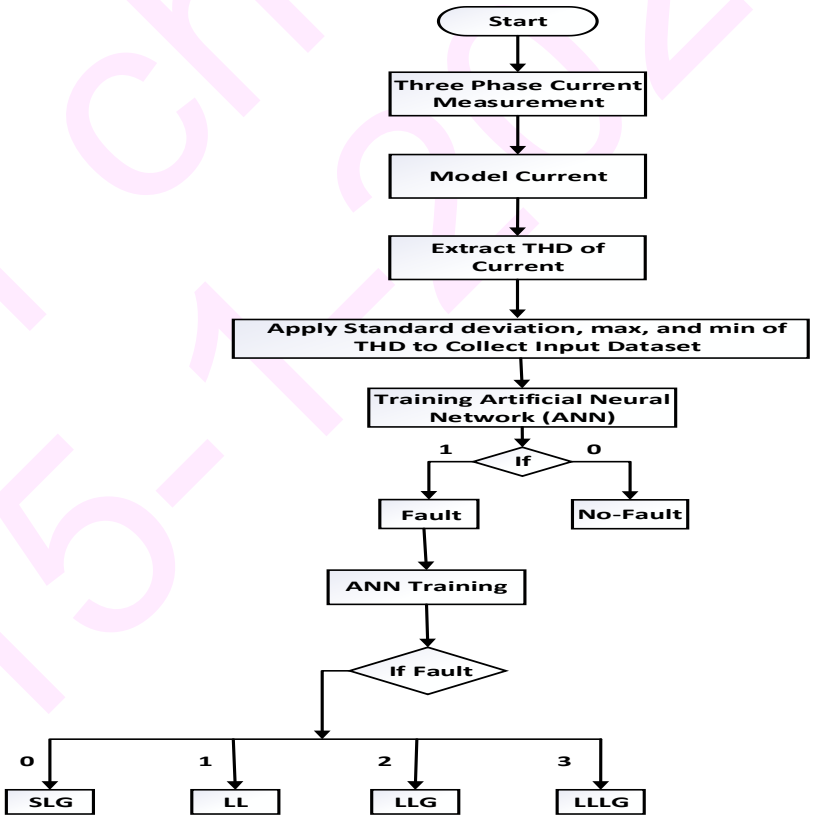

Fig 4.1 Flow Chart for Protection Scheme

For checking 15-12-2024

4.2 Results for PV Array

Voltage calculation: In solar panels voltage is added by connecting panels in series.

Panels in series= 26

$$\text{Voltage} = \text{per panels voltage} * \text{number of panel}$$

$$\text{Total Voltage} = 32.6 * 26 = 847.6\text{V}$$

Current Calculation: In solar panels current is added by connecting panels in parallel.

Panels in parallel= 40

$$\text{Current} = \text{per panels Current} * \text{number of panel}$$

$$\text{Total Current} = 9.2 * 40 = 368\text{A}$$

Power Calculation:

$$\text{Total Voltage} * \text{Total Current} = 847.6\text{V} * 368\text{A} = 311.917\text{KW}$$

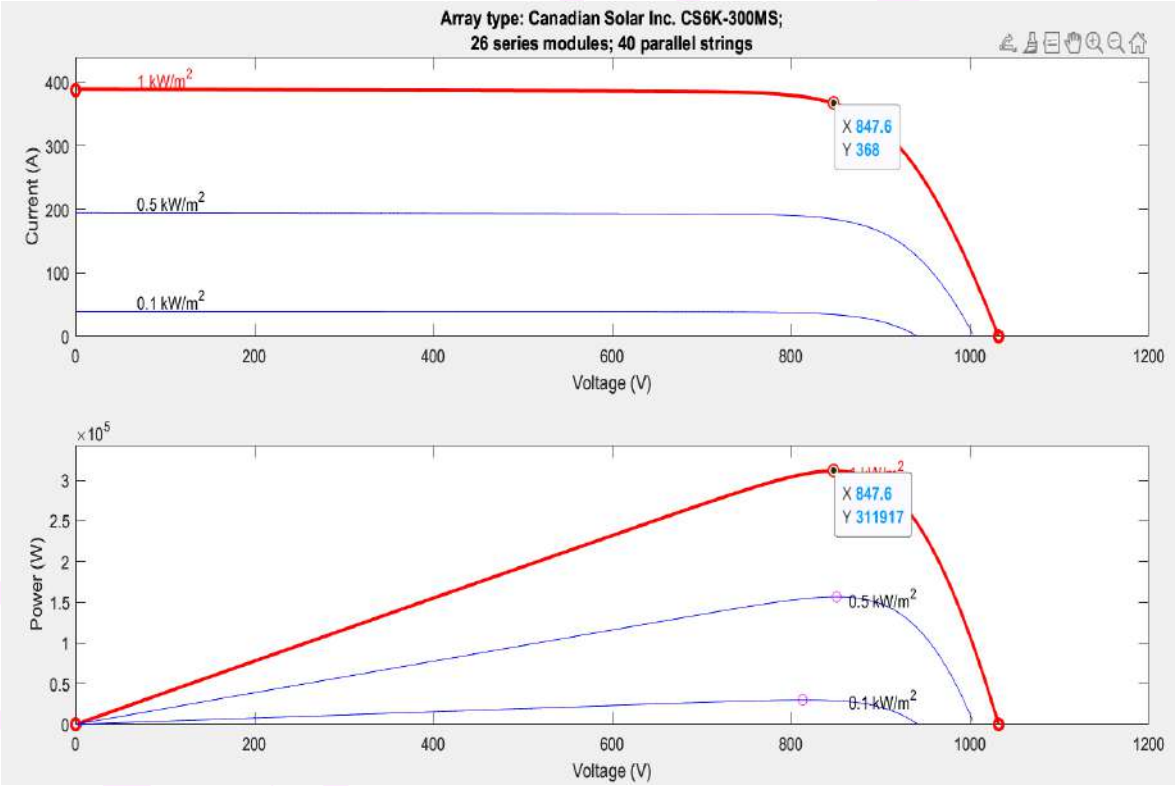

Fig 4.2 PV array output voltage and power

4.3 Results for Phase voltage and current

This Fig 4.3 shows that the output of pv system voltage and current measurement.

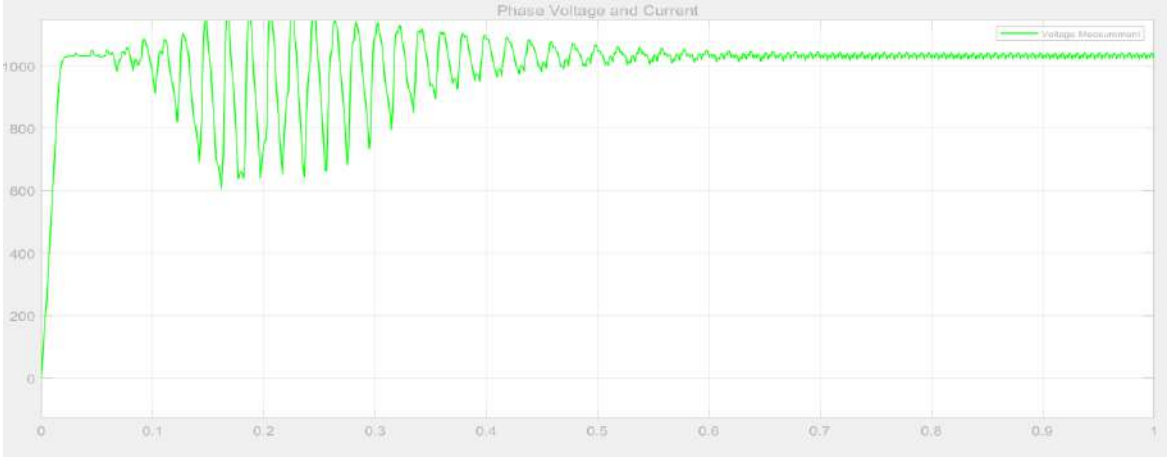

Fig 4.3 Phase voltage and current

4.4 Results for DC/AC Inverter

The output voltage and current of the DC/AC inverter as displayed in Fig 4.4 Where the voltage is measured, the condition is one of distortion-free, smooth LCL filter. Current exhibits distortion in the wave form prior to the LCL filter. 500V of controlled voltage is produced at the inverter side.

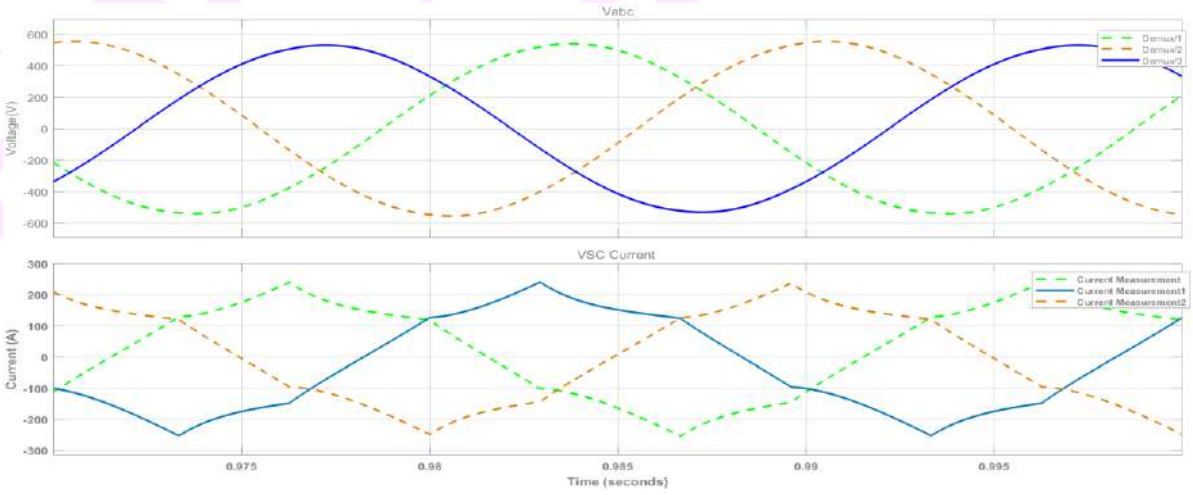

Fig 4.4 DC/AC Inverter

The LCL filter produces a smooth, distortion-free current, as shown in Fig 4.5which, through DG synchronization with the modified IEEE-13 node system, is further connected to the modified IEEE-13 node test system.

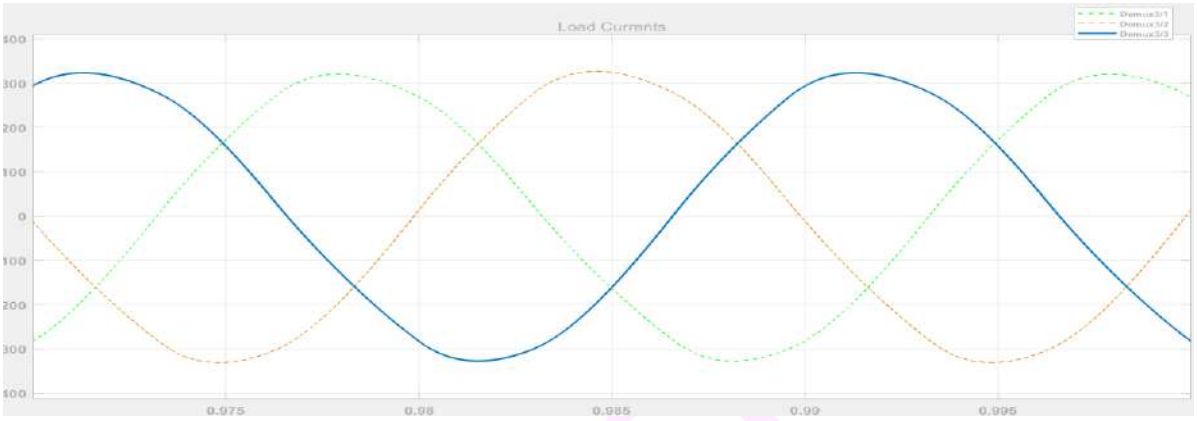

Fig 4.5 Current after LCL filter

4.5 Results for Grid Synchronization

Four essential requirements must be satisfied in order to synchronize a three-phase inverter with the grid network: the phase angle, frequency, voltage magnitude, and phase sequence of the inverter and grid voltages must be equal. The voltage of the grid and inverter are measured as in Fig 4.6, and the output result demonstrates that the four conditions have synchronized the grid and inverter's three phases.

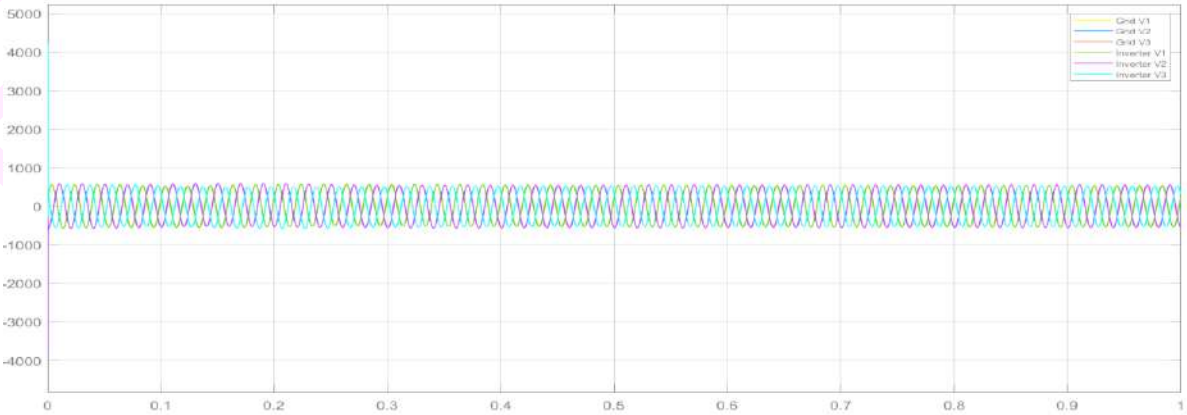

Fig 4.6 Grid Synchronization

For check 2024

4.6 Results for Test Network

The input current is measured and displayed in Fig 4.7, where the test network's behavior is observed under normal conditions and no faults are occurring. The input current waveform is not distorted and has a normal waveform.

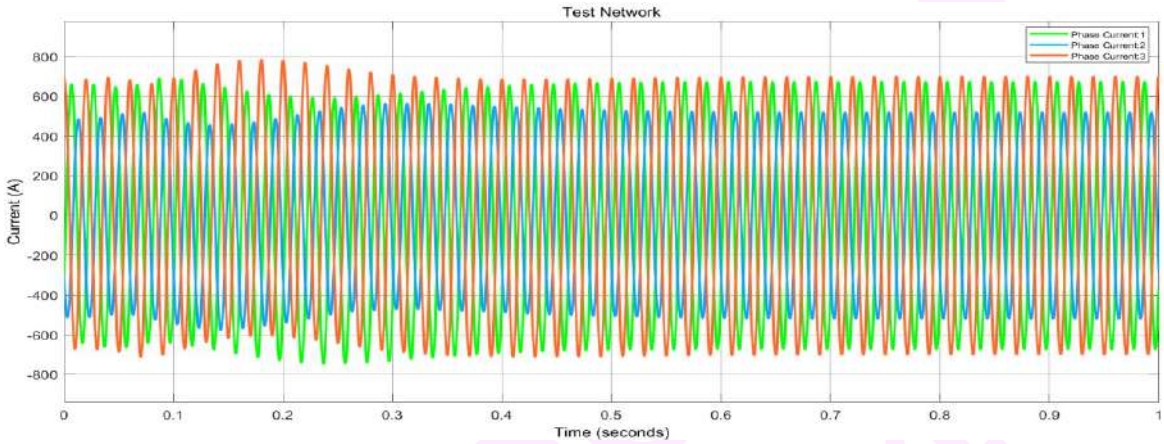

Fig 4.7 Test Network

In Fig 4.8, the measured input current provides a comprehensive view of the test network's behavior, particularly in the absence of any occurring faults but under abnormal or islanded conditions. The observed distortion in the input current waveform is attributed to the dynamic changes in the load. This distortion highlights the system's response to shifts in operational conditions, emphasizing the significance of monitoring and analyzing current characteristics during islanded scenarios. The presence of load-induced variations underscores the complexity of managing the MG in isolation from the main grid.

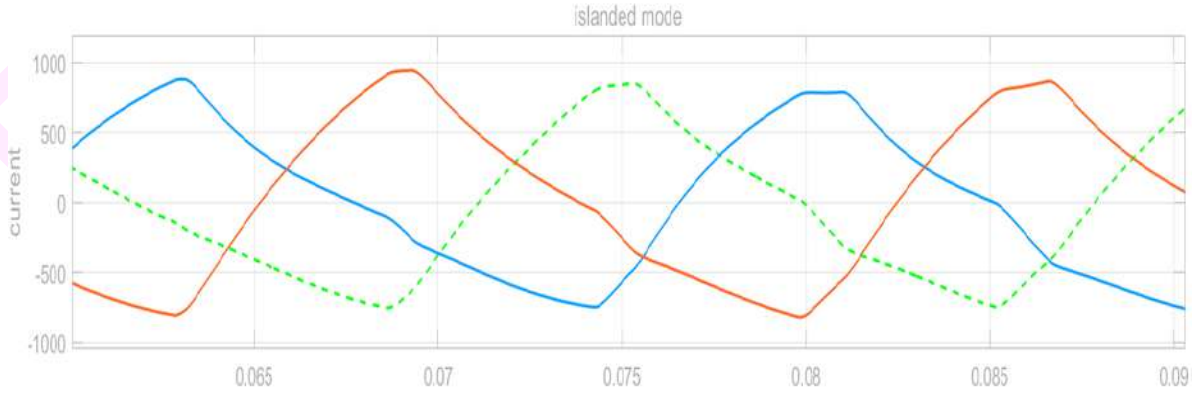

Fig 4.8 Islanded mode

Fig 4.9 provides a detailed depiction of the measured input current as the test network undergoes scrutiny under normal conditions while experiencing a single-phase to ground fault. Within this scenario, the switching time for the single-phase to ground fault ranges between $(0.02\ to\ 0.06\ )sec$, with a corresponding fault resistance of 0.001Ω. The observed behavior of the input current during this fault event offers valuable insights into the network's response dynamics, facilitating a comprehensive understanding of the system's performance under fault conditions.

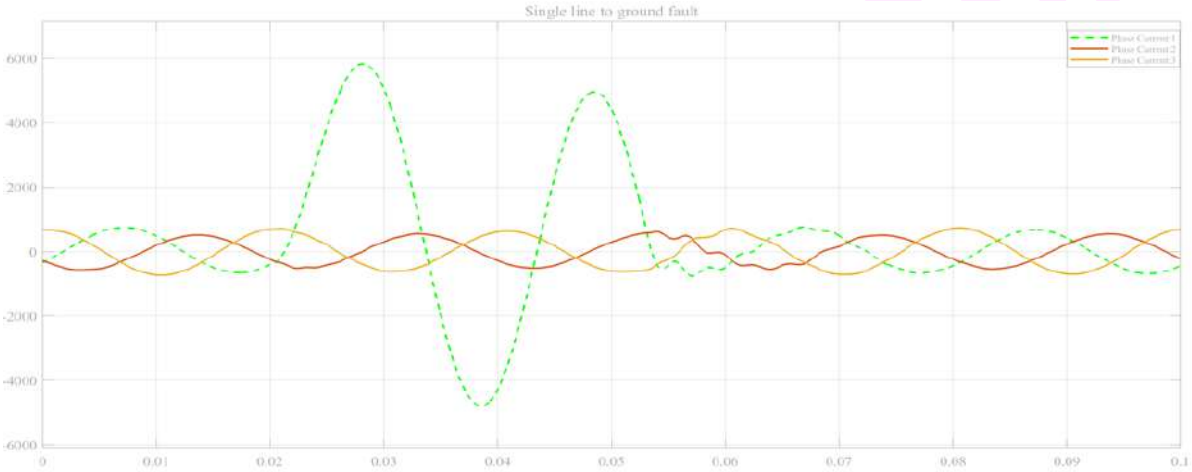

Fig 4.9 Single line to ground fault

Fig 4.10 the measured input current is meticulously illustrated as the test network undergoes examination under typical operating conditions while encountering a line-to-line fault. Within this specific scenario, the switching time for the line-to-line fault varies from$(0.02\ to\ 0.06)\ sec$, accompanied by a fault resistance of 0.001Ω. The detailed depiction of the input current's behavior during this fault occurrence provides valuable insights into the dynamic response of the network.

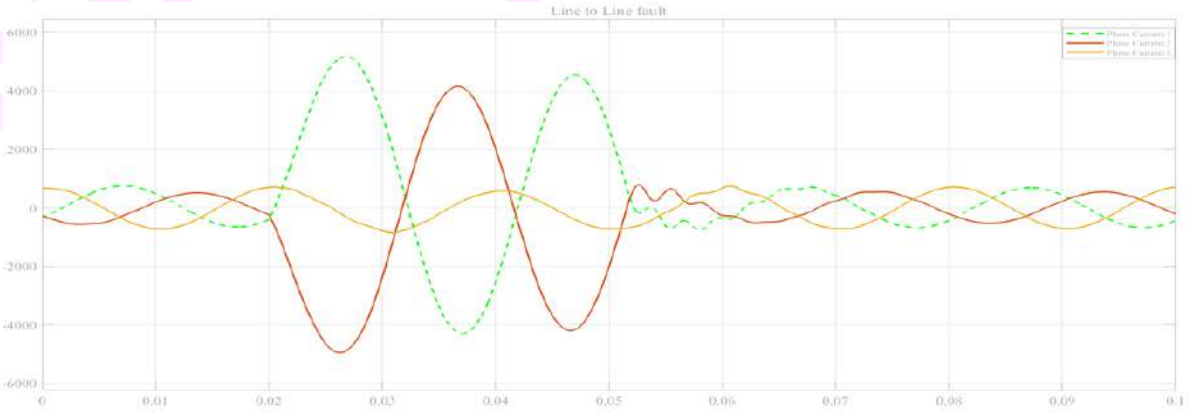

Fig 4.10 Line to line fault

4.7 Results for Modal Current

In Fig 4.11 modal current is created by appropriately combining three-phase currents linearly. It is necessary to consider the currents in all three-phases since TL faults can arise in any of the three phases. Three-phase currents can be transformed into a modal signal to reduce memory usage and computation time.

A modal current is the main signal used in the defect detection process. The following examples demonstrate how the modal signal can be created by correctly combining the three-phase voltage or current signals in a linear fashion.

$$Im = \alpha I_a + \beta I_b + \gamma I_c \ldots\ldots\ldots\ldots\ldots\ldots\ldots\ldots (3.20)$$

$$Vm = \alpha V_a + \beta V_b + \gamma V_c \ldots\ldots\ldots\ldots\ldots\ldots\ldots\ldots (3.21)$$

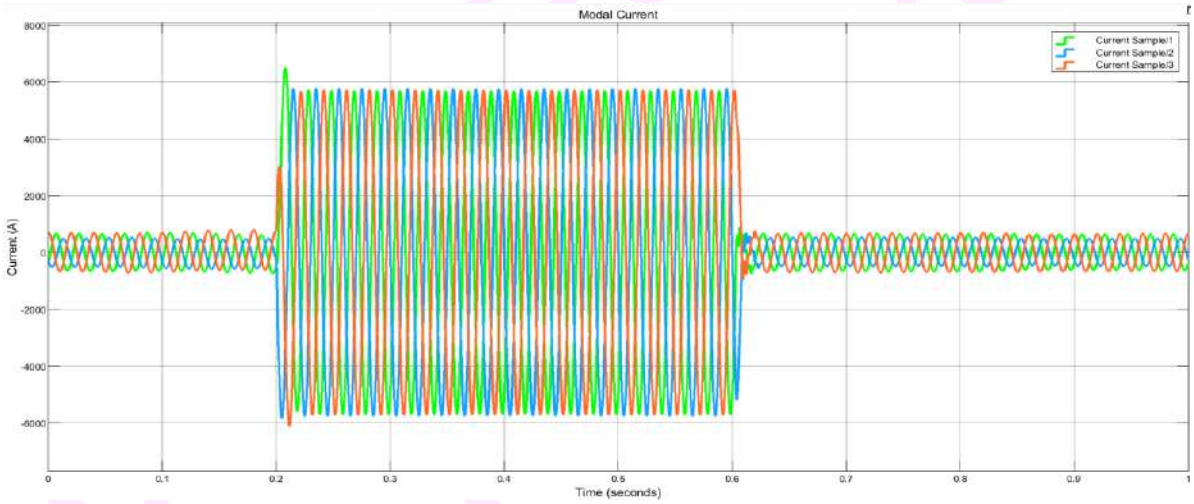

Fig 4.11 Modal Current

4.8 Results for Wavelet Transform

In Fig 4.12, the wavelet transform (WT) is employed to analyze power systems, proving invaluable for tasks such as power system protection, ensuring the quality of power, and detecting partial discharges. Unlike the Fourier transform (FT), which transforms a signal from its behavior over time to its frequency components, the WT provides insight into both the frequency and time aspects of a signal. In our simulation, where the power system is interconnected with the grid, we are

investigating how the WT can enhance our understanding. The switching time for faults has been set between $(0.02\ to\ 0.06)$ sec, with the fault resistance maintained at 0.001 ohms.

$$X_f = \int_{-\infty}^{\infty} x(t)e^{-j2\pi ft}dt \ldots\ldots\ldots\ldots\ldots\ldots (3.22)$$

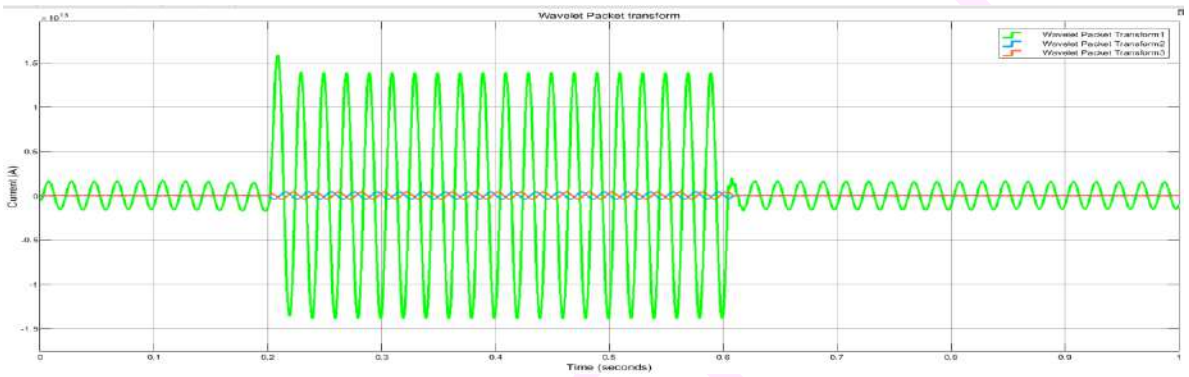

Fig 4.12 Modal Current

4.9 Results for Total Harmonic Distortion of Current

In Fig 4.13 signal distortion is indicated by THD. It is regarded as a sensitive feature against the fault and raises the harmonics. It can be current harmonics and is defined as the ratio of total harmonics to the fundamental frequency. The THD of current is calculated with the use of equations and.

$$THD_i = \frac{\sqrt{{I_1}^2+{I_2}^2+{I_3}^2+\cdots{I_n}^2}}{I_1} \ldots\ldots\ldots\ldots\ldots\ldots\ldots\ldots (3.24)$$

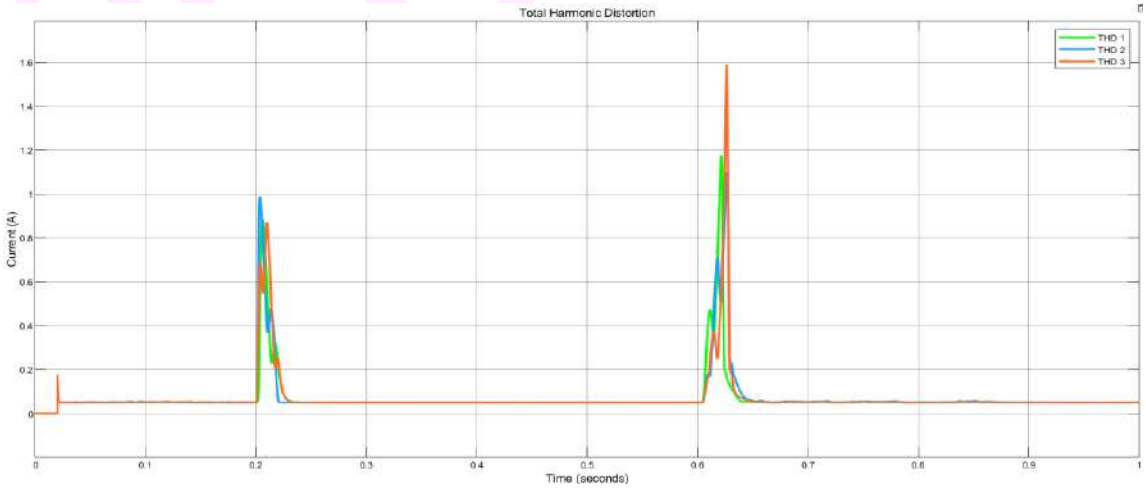

Fig 4.13 Total harmonic distortion

4.10 Results for Artificial Neural Network

The cross-validation technique is used to help the ANN classifier's ability to be more widely applied. The simulated data that is available for cross-validation is split into two sets: the first is the training set, which is used to train the ANN and set its parameters. The remaining examples are test cases, meaning that fresh examples are used to test the algorithm. To determine accuracy, the trained ANN's prediction is compared to the test example's original label.

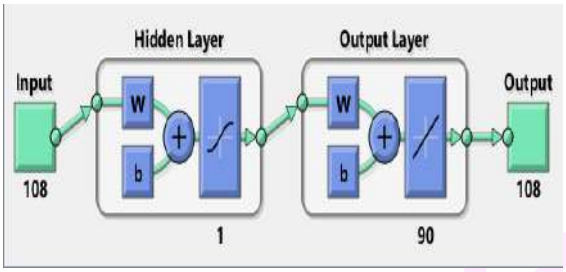

Fig 4.14 ANN Architecture

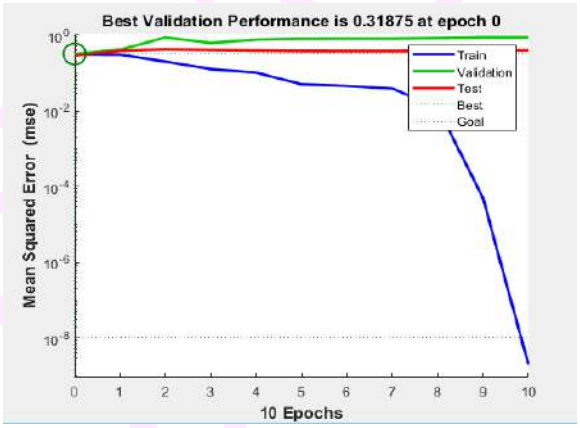

Fig 4.15 ANN Best Validation

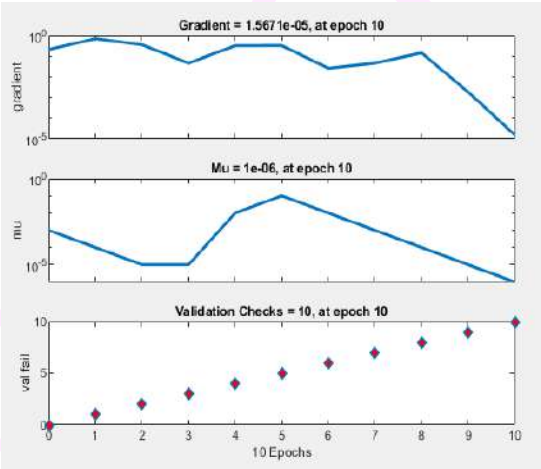

Fig 4.16 ANN performance

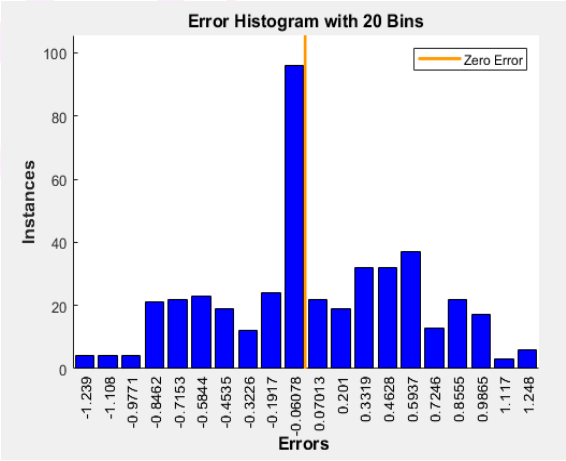

Fig 4.17 ANN Error Histogram

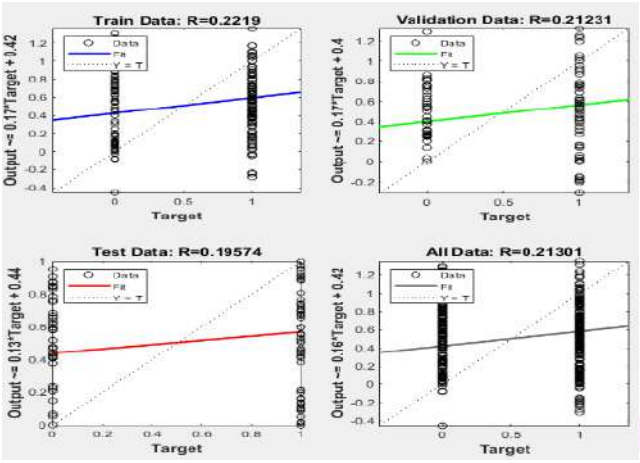

Fig 4.18 ANN Training Data

Column1	Column2	Column3	Column4
TrueLabel	Predicated Label	Score	Fault_line
1	1	-2.8577	phase_A
0	0	1	phase_B
1	1	-2.8577	phase_C
1	1	-3.8379	Neutral
0	0	1	phase_C
1	0	0.99978	phase_A
0	0	1	phase_C
1	0	0.999984	Neutral
0	0	0.9999	phase_B
1	0	0.99984	Neutral

Fig 4.19 ANN True and Predicated Label

In ANN training and testing Data I have selected 108 data randomly to train ANN. And give accuracy about 75%

For check 15-1-2024

Chapter 5

Conclusion

Many strategies, including communication-based, active, and passive methods, have been put forth to identify islanding. When there is a power imbalance between the power generated by the distributed generator and the power consumed by the load, passive techniques are effective. Conversely, active techniques degrade the quality of the power and are less effective when there are several DGs present. Communication-based islanding detection methods are expensive and complicated even though they lack NDZ methods. Through computer simulation, the effectiveness of a widely-used passive anti-islanding method was confirmed. This thesis examines a passive anti-islanding scheme for harmonic detection (DH). It is challenging to choose a threshold for the DH method that will detect islanding without causing false trips or failing to distinguish between different types of disturbances. This method should be used in conjunction with other methods in the distribution network as it is not sufficient to identify islanding on its own.

The hybrid distribution system successfully employed an islanding technique based on WT-ANN. The wavelet transform can split up voltage signals into various frequency ranges. It can be applied to the acquisition of negative sequence voltage signals to extract discriminative features. After that, an ANN that has been trained to distinguish between islanding and non-islanding events is fed the energy content and standard deviation of the wavelet details. The quality of the WT indices obtained is validated by the high accuracy of ANN.

The power industry can now apply machine learning in a feasible and user-friendly way by utilizing Microsoft Azure Machine Learning Studio to implement the WT-ANN based anti-islanding technique. The trained model can be accessed from multiple locations and devices simultaneously by being deployed as a Web Service. It is practically feasible to monitor the system continuously and more accurately. With a lower implementation cost, this offers a promising future for power system control and detection.

For checking 15-1-2024

5.1 Future Work

Despite producing a very high accuracy rate, the suggested method's validation was done on a small testing set. A larger testing data set will yield a recognition rate that is more accurate and general. One system configuration was used to test the suggested technique. Comparable simulations with alternative system models could be run to boost confidence in these findings. Putting the suggested strategy into practice and verifying it in real time is another avenue for future research. Research on WT's subpar performance during voltage swell events is also.

For checking 15-1-2024

REFERENCES

[1] T. Adefarati and R.C. Bansal, "Integration of renewable distributed generators into the distribution system," *IET Renewable Power Generation,* p. 12, 22nd February 2016.

[2] Faisal Mumtaz and Islam Safak Bayram , "Planning, Operation, and Protection of Microgrids," *3rd International Conference on Energy and Environment Research,* pp. 1-7, 11 September 2016.

[3] A. Aithal, Gen Li, Jianzhong Wu and James Yu, "Performance of an electrical distribution network with Soft Open Point during a grid side AC fault," *http://www.elsevier.com/locate/apenergy,* pp. 1-11, 13 August 2017.

[4] Lukasz Staszewski, Zbigniew Leonowicz and Sunny Katyara, "Protection Coordination of Properly Sized and Placed Distributed Generations–Methods," *Faculty of Electrical Engineering, Sukkur IBA University,* pp. 1-22, 8 October 2018.

[5] S. A. M. Javadian and Maryam Massaeli, "An adaptive overcurrent protection scheme for distribution networks including DG using distribution automation system and its implementation on a real distribution network," *Indian Journal of Science and Technology ,* pp. 1-8, Nov 2011.

[6] S. R. Salkuti, "Challenges, issues and opportunities for the development of smart grid," *International Journal of Electrical and Computer Engineering (IJECE) ,* Vols. Vol. 10, No. 2, April 2020, pp. 1179~1186, pp. 1-8, Oct 10, 2019 .

[7] L. Strezoski, Harsha Padullaparti, Fei Ding and Murali Baggu, "Integration of Utility Distributed Energy Resource Management System and Aggregators for Evolving Distribution System Operators," *JOURNAL OF MODERN POWER SYSTEMS AND CLEAN ENERGY,* Vols. VOL. 10, NO. 2, pp. 1-9, March 2022.

[8] Sanjeevikumar Padmanaban, Seyfettin Vadi, Ramazan Bayindir, Frede Blaabjerg and Lucian Mihet-Popa, "Optimization and Control Methods Used to Provide Transient Stability in Microgrids," *energies,* pp. 1-20, 19 September 2019.

[9] S. Beheshtaein, Robert Cuzner, Mehdi Savaghebi and Josep M. Guerrero, "Review on microgrids protection," *IET Generation, Transmission & Distribution,* pp. 1-17, 1st February 2019.

[10] S. Vadi, Sanjeevikumar Padmanaban, Ramazan Bayindir, Frede Blaabjerg and Lucian Mihet-Popa, "A Review on Optimization and Control Methods Used to Provide Transient Stability in Microgrids," *energies,* pp. 1-20, 19 September 2019.

Forthcoming 2024

[11] R. Sitharthan, M. Geethanjali and T. K. S. Pandy, "Adaptive protection scheme for smart microgrid with electronically coupled distributed generations," *Alexandria Engineering Journal,* pp. 1-12, 27 June 2016.

[12] Alexandre Oudalov and Antonio Fidigatti, "ADAPTIVE NETWORK PROTECTION IN MICROGRIDS," *Int. J. Distrib.Energy.Resour.,* Vols. vol. 5, no, 3, pp. 1-24, 2009.

[13] Mostafa Bakkar, S. Bogarra, F. Córcoles and J. Iglesias, "Overcurrent protection based on ANNs for smart distribution networks with grid-connected VSIs," *IET Generation, Transmission & Distribution,* pp. 1-16, 27 October 2020.

[14] Patrick Tendayi Manditereza and Ramesh C. Bansal, "Fault detection and location algorithm for DG-integrated distribution system," *The Journal of Engineering,* pp. 1-5, 23rd May 2018.

[15] R. Sitharthan, M. Geethanjali and T. Karpaga Senthil Pandy, "Adaptive protection scheme for smart microgrid with electronically coupled distributed generations," *Alexandria Engineering Journal,* pp. 1-12, 27 June 2016.

[16] Zaid Alhadrawi, Mohd Noor Abduallah and Hazlie Mokhlis, "Review of microgrid protection strategies: current status and future prospects," *TELKOMNIKA Telecommunication Computing Electronics and Control,* Vols. Vol. 20, No. 1, February 2022, pp. 173~184, pp. 1-12, Dec 25, 2021.

[17] K. R. Bharath, M. Krishnan Mithun and P. Kanakasabapathy, "A Review on DC Microgrid Control Techniques, Applications and Trends," *INTERNATIONAL JOURNAL of RENEWABLE ENERGY RESEARCH,* Vols. Vol.9, No.3, pp. 1-11, 14.08.2019.

[18] E. Abbaspour, B. Fani, E. Heydarian-Forushani and A. Al-Sumaiti, "A multi-agent based protection in distribution networks including distributed generations," *7th International Conference on Green Energy Technologies,* pp. 1-12, 22 October 2022.

[19] FAHD AMIN HARIR, "PROTECTION OF MODERN DISTRIBUTION SYSTEMS," *MISSOURI UNIVERSITY OF SCIENCE AND TECHNOLOGY,* pp. 1-20, 2021.

[20] Łukasz Huchel and Hatem H. Zeineldin, "Planning the Coordination of Directional Overcurrent Relays for Distribution Systems Considering DG," *IEEE TRANSACTIONS ON SMART GRID,* pp. 1-8, 2015.

[21] A. A. Salam, A. Mohamed and M. A. Hannan, "TECHNICAL CHALLENGES ON MICROGRIDS," *ARPN Journal of Engineering and Applied Sciences ,* Vols. VOL. 3, NO. 6, pp. 1-6, 2008.

[22] Swetalina Sarangi, Binod Kumar Sahu and Pravat Kumar Rout, "A comprehensive review of distribution generation integrated DC microgrid protection: issues, strategies, and future direction," *REVIEW PAPER,* pp. 1-26, 23 October 2020.

For Checking

[23] Ali Agheli, Hossein Askarian Abyaneh, Reza Mohammadi Chabanloo and Hamed Hashemi Dezaki, "Reducing the Impact of DG in Distribution Networks Protection Using Fault Current Limiters," *The 4th International Power Engineering and Optimization Conf. (PEOCO2010), Shah Alam, Selangor, MALAYSIA,* pp. 1-7, 23-24 June 2010.

[24] Walid El-Khattam and Tarlochan S. Sidhu, "Restoration of Directional Overcurrent Relay Coordination in Distributed Generation Systems Utilizing Fault Current Limiter," *IEEE TRANSACTIONS ON POWER DELIVERY,* Vols. VOL. 23, NO. 2, pp. 1-10, APRIL 2008.

[25] Taha Selim Ustun, Cagil Ozansoy and Aladin Zayegh, "A Central Microgrid Protection System for Networks with Fault Current Limiters," *School of Engineering and Science, Victoria University Melbourne, Australia,* pp. 1-4, 2011.

[26] B. Abdi, M. Abroshan, M. H. Aslinezhad and A. Alimardani, "Coordination Return of Protective Devices in Distribution Systems in Presence of Distributed Generation," *ICSGCE,* pp. 1-8, September 2011.

[27] R.M. Chabanloo, H.A. Abyaneh, A. Agheli and H. Rastegar, "Overcurrent relays coordination considering transient behaviour of fault current limiter and distributed generation in distribution power network," *IET Generation, Transmission & Distribution,* pp. 1-9, 2011.

[28] Hassan Nikkhajoei and Robert H. Lasseter, "Microgrid Fault Protection Based on Symmetrical and Differential Current Components," *Consortium for Electric Reliability Technology Solutions,* pp. 1-72, December 2006.

[29] R. J. Best, M. D. J and C. P. A, "Communication assisted protection selectivity for reconfigurable and islanded power networks," *International Universities Power Engineering Conference (UPEC),* pp. 1-6, 2009.

[30] M. Amin Zamani, Amirnaser Yazdani and Tarlochan S. Sidhu, "A Communication-Assisted Protection Strategy for Inverter-Based Medium-Voltage Microgrids," *IEEE TRANSACTIONS ON SMART GRID,,* Vols. VOL. 3, NO. 4, pp. 1-12, DECEMBER 2012.

[31] Susmita Kar, S. R. Samantaray and M. Dadash Zadeh, "Data-Mining Model Based Intelligent Differential Microgrid Protection Scheme," *IEEE SYSTEMS JOURNAL,* pp. 1-10, 2014.

[32] J. A. Peças Lopes, C. L. Moreira and A. G. Madureira, "Defining Control Strategies for MicroGrids Islanded Operation," *IEEE TRANSACTIONS ON POWER SYSTEMS,* Vols. VOL. 21, NO. 2, pp. 1-9, 2006.

[33] Syed Basit Ali Bukhari, Raza Haider, Muhammad Saeed Uz Zaman, Yun-Sik Oh, Gyu-Jung Cho and Chul-Hwan Kim, "An interval type-2 fuzzy logic based strategy for microgrid protection," *Electrical Power and Energy Systems ,* vol. vol.98, pp. 1-10, 29 November 2017.

[34] P. W. Lehn, "Exact Modeling of the Voltage Source Converter," *IEEE TRANSACTIONS ON POWER DELIVERY,* Vols. VOL. 17, NO. 1, pp. 1-6, 2002.

[35] Mustafa DURSUN and M. Kenan DÖŞOĞLU , "LCL Filter Design for Grid Connected Three-Phase Inverter," *IEEE,* pp. 1-5, 2018.

[36] Raza Haider, Chul Hwan Kim, Teymoor Ghanbari, Syed Basit Ali Bukhari, Muhammad Saeed uz Zaman, Shazia Baloch and Yun Sik Oh, "Passive islanding detection scheme based on autocorrelation function of modal current envelope for photovoltaic units," *IET Generation, Transmission & Distribution,* Vols. Vol. 12 Iss. 3, pp. 726-736, pp. 1-11, 2017.

[37] Anamika Yadav and Yajnaseni Dash, "An Overview of Transmission Line Protection by Artificial Neural Network: Fault Detection, Fault Classification, Fault Location, and Fault Direction Discrimination," *Hindawi Publishing Corporation,* pp. 1-21, 2014.

[38] Mr. Ashwin K V, Mr. Venkata Satya Rahul Kosuru, Mr. Sridhar S and Mr. P. Rajesh, "A Passive Islanding Detection Technique Based on Susceptible Power Indices with Zero Non-Detection Zone Using a Hybrid Technique," *International Journal of INTELLIGENT SYSTEMS AND APPLICATIONS IN ENGINEERING,* pp. 1-13, 10/02/2023.

[39] Amany M. El-Zonkoly, "Fault Diagnosis in Distribution Networks with Distributed Generation," *Smart Grid and Renewable Energy,* pp. 1-11, 2010.

[40] Bogdan Betea, Petru Dobra, Mircea-Cristian Gherman and Liviu Tomesc, "Comparison between envelope detection methods for bearing defects diagnose," *2nd IFAC Workshop on Convergence of Information Technologies and Control Methods with Power Systems,* pp. 1-6, 2013.

[41] Mohammad Amin Jarrahi, Haidar Samet and Teymoor Ghanbari, "Fast Current-Only Based Fault Detection Method in Transmission Line," *IEEE SYSTEMS JOURNAL,* pp. 1-12, 2018.

[42] X. Li, A. Dyśko and G. Burt, "Traveling Wave Based Protection Scheme for Inverter Dominated Microgrid Using Mathematical Morphology," *IEEE,* Vols. vol. 5, no. 5, pp. 1-8, 2014.

For Checking 15-1-2024

Plagiarism Report

ORIGINALITY REPORT

19%	11%	16%	8%
SIMILARITY INDEX	INTERNET SOURCES	PUBLICATIONS	STUDENT PAPERS

PRIMARY SOURCES

1	epdf.pub Internet Source	3%
2	dspace.aus.edu:8443 Internet Source	2%
3	Submitted to Higher Education Commission Pakistan Student Paper	1%
4	Hosseini, Seyed Amir, Hossein Askarian Abyaneh, Seyed Hossein Hesamedin Sadeghi, Farzad Razavi, and Adel Nasiri. "An overview of microgrid protection methods and the factors involved", Renewable and Sustainable Energy Reviews, 2016. Publication	1%
5	Amirnaser Yazdani, Reza Iravani. "Voltage-Sourced Converters in Power Systems", Wiley, 2010 Publication	1%
6	Submitted to University of Wollongong Student Paper	1%